GEOLOGIC NOTE

Controls on fluviolacustrine reservoir distribution and architecture in passive salt-diapir provinces: Insights from outcrop analogs

Wendy J. Matthews, Gary J. Hampson, Bruce D. Trudgill, and John R. Underhill

ABSTRACT

Fluviolacustrine strata host significant hydrocarbon volumes in basins characterized by syndepositional growth of passive salt diapirs. An understanding of salt-sediment interaction is critical to the prediction of reservoir distribution and architecture in these strata. Large-scale stratal geometries and thickness changes resulting from salt movement are commonly apparent on seismic data, but to date, there are few predictive models for facies architecture at subseismic, reservoir scale.

This article uses a high-quality outcrop data set of fluviolacustrine strata in an exhumed salt basin (Upper Triassic Chinle Formation, Paradox Basin, Utah) as an analog for improved understanding of subsurface data sets of similar structural and sedimentological setting. Salt-sediment interaction in the Chinle Formation is expressed by localized lateral variations in stratigraphic thickness, angular stratal relationships, and changes in facies architecture. Based on these criteria, there is evidence for salt-sediment interaction across a series of syndepositional salt structures, including anticlines above buried salt pillows, salt walls exposed at surface, and salt-withdrawal minibasins. Stratigraphy and facies architecture across these structures reflect the following controls: regional subsidence, localized differential accommodation space, and localized paleogeomorphology. Both localized controls were driven by syndepositional salt movement, which exhibited subtle spatial and temporal variations

Manuscript received October 21, 2006; provisional acceptance February 28, 2007; revised manuscript received April 12, 2007; final acceptance May 31, 2007.
DOI:10.1306/05310706123

AUTHORS

WENDY J. MATTHEWS ~ *Department of Earth Science and Engineering, Imperial College London, South Kensington Campus, London SW7 2AZ, United Kingdom; present address: Exploration and Production Technology Group, BP plc, Chertsey Road, Sunbury-on-Thames, Middlesex TW16 7LN, United Kingdom; wendy.matthews@uk.bp.com*

Wendy Matthews is currently a sedimentologist with the Exploration and Production Technology Group at BP, where her work involves sedimentary geology research and global technical consulting. She received her B.Sc. and M.Sc. degrees from the University of Sheffield and the University of Aberdeen, respectively. The research for this article was conducted as part of her Ph.D. at Imperial College London.

GARY J. HAMPSON ~ *Department of Earth Science and Engineering, Imperial College London, South Kensington Campus, London SW7 2AZ, United Kingdom; g.j.hampson@imperial.ac.uk*

Gary Hampson is senior lecturer in sedimentary geology at Imperial College London. He earned his B.A. degree in natural sciences from the University of Cambridge (1991) and his Ph.D. in sedimentology and sequence stratigraphy from the University of Liverpool (1995). His research interests lie in the understanding of siliciclastic depositional systems and their preserved stratigraphy and in applying this knowledge to reservoir characterization.

BRUCE D. TRUDGILL ~ *Department of Geology and Geological Engineering, Colorado School of Mines, Golden, Colorado 80401-1877*

Bruce Trudgill received a B.Sc. degree from the University of Wales, Aberystwyth, and a Ph.D. in structural geology from Imperial College London. He is currently an associate professor in the Department of Geology and Geological Engineering at the Colorado School of Mines. His current interests are in the growth of fault arrays, salt tectonics, and structural controls on depositional systems.

JOHN R. UNDERHILL ~ *School of Geosciences, University of Edinburgh, The Kings Buildings, West Main Road, Edinburgh EH9 3JG, United Kingdom*

John Underhill holds a B.Sc. degree in geology from Bristol University and a Ph.D. from the University of Wales. He worked for Shell International before moving to Edinburgh University in 1989, where he holds the Chair of Stratigraphy. John has twice been awarded the European Association of Petroleum Geoscientists Distinguished Lecturer Award, has won the AAPG Matson Award, and has also been an AAPG Distinguished Lecturer. John's current primary research focus is on understanding the function of salt in the tectonic development and evolution of sedimentary basins.

ACKNOWLEDGEMENTS

We thank the United Kingdom Natural Environment Research Council and Total for supporting this research and in particular Lutz Seiffert, Neville Taylor, and Jonathan Wonham. Our ideas evolved via fruitful discussions with Nick Banbury, Russell Dubiel, Steve Hasiotis, Chris Jackson, Howard Johnson, Mary Kraus, Asisat Lamina, Spencer Lucas, Proscovia Nabbanja, Shane Prochnow, and Mark Rowan. We also thank Jim and Leigh at Roadrunner and Bruce and Cindy at Grand View for their hospitality in the field and Robert Leckenby and Neil Hurley for help in acquiring outcrop gamma-ray data. This article has benefited from the thorough reviews and editorial comments of Carol Christopher, Ernest Mancini, Andrew Miall, Richard Moiola, Donald Owen, and Howard White.

during the deposition of the Chinle Formation. The outcrop data set is used to develop generic predictive models of facies distributions and architectures resulting from different conditions of regional tectonic subsidence and/or fluvial energy. Analysis of stratigraphic expansion across syndepositional passive diapirs suggests that the outcrop-derived models are applicable to many subsurface data sets.

INTRODUCTION

Prediction of reservoir distribution and architecture in salt basins is extremely challenging because of the wide range of potential tectonostratigraphic controls on facies distribution and of the interplay between these controls (e.g., Smith et al., 1993; Barde et al., 2002b). Salt-sediment interaction occurs at a range of spatial and temporal scales, and it controls (1) the structural style in the subsurface; (2) the geomorphic processes at the surface; and (3) the thickness, stratal architecture, and facies distributions in the stratigraphic record (e.g., Barton, 1933; Vendeville and Jackson, 1991; Barde et al., 2002a; Giles and Lawton, 2002; Rowan et al., 2003). Feedback between these three components is common (e.g., rapid sedimentation may drive loading of subsurface salt, which in turn produces a geomorphic low to accommodate further sediment). The problem of understanding a complex system is exacerbated in many petroliferous basins by poor seismic imaging of steeply dipping strata adjacent to complicated salt-overburden contacts. Outcrop analogs from exposed salt basins provide a unique tool to resolve these problems because they provide a high-resolution (subseismic) record of depositional processes, facies distributions, and stratal geometries at reservoir scale. Such outcrop analogs are rare (e.g., La Popa Basin, Mexico; Giles and Lawton, 2002; Rowan et al., 2003; Aschoff and Giles, 2005; Shelley and Lawton, 2005), but potentially critical in reducing exploration risk and maximizing production efficiency from salt-related reservoirs.

In this article, we document detailed stratigraphic relationships and facies architectures influenced by salt-sediment interaction from extensive three-dimensional exposures of fluviolacustrine strata in the Upper Triassic Chinle Formation, northeastern Paradox Basin, Utah. These strata provide generic, predictive insights into the function of syndepositional salt movement in controlling reservoir distribution and architecture. We summarize and extend an existing, preliminary tectonostratigraphic synthesis for the Chinle Formation in the northeastern Paradox Basin (Matthews et al., 2004), which we then use to examine the controls on reservoir-scale facies architecture. The specific aims of the article are (1) to document the evidence of syndepositional salt tectonism across a complex, three-dimensional array of salt structures; (2) to evaluate regional, subregional, and local controls on stratigraphy in an evolving salt basin; and (3) to develop refined generic models for fluviolacustrine strata in salt basins.

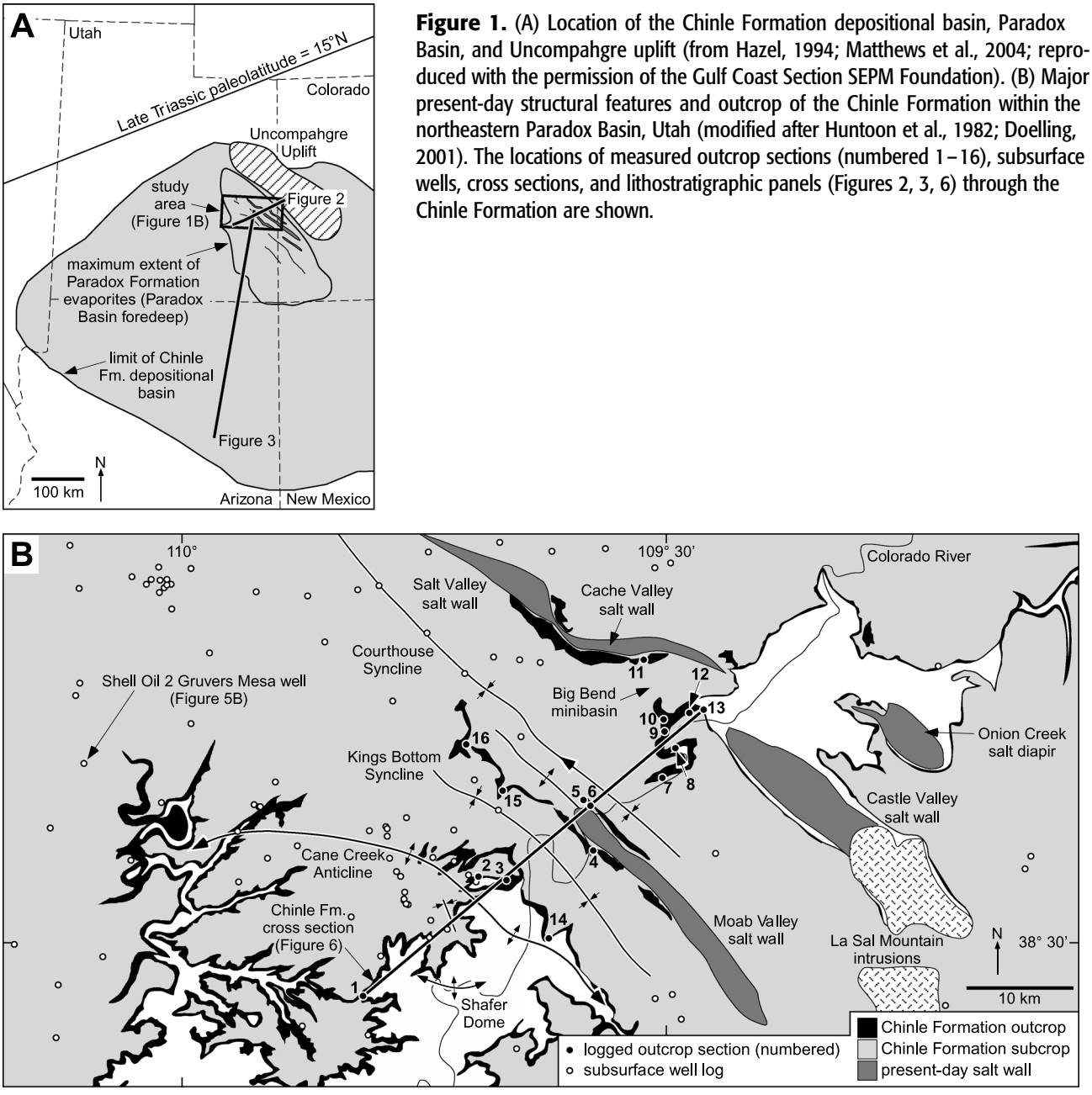

Figure 1. (A) Location of the Chinle Formation depositional basin, Paradox Basin, and Uncompahgre uplift (from Hazel, 1994; Matthews et al., 2004; reproduced with the permission of the Gulf Coast Section SEPM Foundation). (B) Major present-day structural features and outcrop of the Chinle Formation within the northeastern Paradox Basin, Utah (modified after Huntoon et al., 1982; Doelling, 2001). The locations of measured outcrop sections (numbered 1–16), subsurface wells, cross sections, and lithostratigraphic panels (Figures 2, 3, 6) through the Chinle Formation are shown.

GEOLOGICAL SETTING OF THE NORTHEASTERN PARADOX BASIN

Basin-Scale Salt Tectonics

The Paradox Basin is a large (190 × 265-km; 118 × 164-mi), asymmetric basin developed along the southwestern margin of the basement-cored Uncompahgre uplift during the Pennsylvanian–Permian Ancestral Rocky Mountain orogeny (Figure 1A) (White and Jacobson, 1983). The Paradox Basin was originally interpreted as a pull-apart basin (Stevenson and Baars, 1986), but a comprehensive recent synthesis (Barbeau, 2003) suggests that the basin kinematics, geometry, and subsidence history are more consistent with an intraforeland basin that formed under the load of the Uncompahgre uplift. The Uncompahgre uplift trends northwest, abuts the deepest part of the Paradox Basin, and is believed to have been the main proximal sediment source for the Pennsylvanian–Triassic sediments within the

northeastern part of the Paradox Basin (e.g., Mack and Rasmussen, 1984). The medial foredeep of the Paradox Basin (sensu Barbeau, 2003; Trudgill et al., 2004) roughly coincides with the depositional extent of salt within the middle Pennsylvanian Paradox Formation, which forms the oldest part of the basin fill.

Salt structures in the Paradox Basin are restricted to the Paradox fold and fault belt, located in the northeastern part of the basin (Kelley, 1958; Doelling, 1988). These structures trend northwest (Figure 1B) and display a variety of structural styles, ranging from deeply buried, nonpiercing salt pillows to salt walls that are exposed at the surface (Figure 2) (Doelling et al., 2002; Trudgill et al., 2004). Since Prommel's (1923) pioneering work in the Paradox Basin, many investigators have documented stratigraphic relationships, which they attributed to syndepositional salt movement: (1) stratigraphic thinning and localized absence of the super-Pennsylvanian formations in proximity to the salt structures; (2) interformational unconformities across the Chinle-Moenkopi and Chinle-Wingate boundaries; and (3) intraformational angular unconformities within the Moenkopi and Chinle formations (Shoemaker and Newman, 1959; Stewart, 1969; Stewart et al., 1972; Blakey and Gubitosa, 1984; Bromley, 1991; Hazel, 1994; Doelling and Ross, 1998; Miall and Arush, 2001; Doelling, 2001, 2002; Doelling et al., 2002; Matthews et al., 2004; Trudgill et al., 2004; Banbury, 2005; Lawton and Buck, 2006).

Salt movement began shortly after or possibly during salt deposition as clastic sediments shed from the rising Uncompahgre uplift infilled the foreland basin during the late Pennsylvanian and differentially loaded the underlying salt layers. In the northeastern part of the basin, salt walls formed in response to progradational sediment loading. The salt walls were elongated by salt flowage against and over deep-seated, northwest-trending basement faults (Trudgill et al., 2004). The most active period of salt movement lasted for approximately 75 m.y. (late Pennsylvanian through Triassic; Doelling, 1988; Trudgill et al., 2004; Banbury, 2005). Minor salt movement continued during the Jurassic and possibly the Cretaceous (Bromley, 1991; Tyler and Etheridge, 1993; Trudgill et al., 2004), and structures were gently tightened during Paleogene (Laramide) compression (Trudgill et al., 2004). Local dissolution and collapse of the salt walls has occurred during Neogene uplift and exposure of the Colorado Plateau (e.g., Doelling and Ross, 1998), which resulted in erosion of more than 3 km (1.8 mi) of overburden from the northeastern Paradox Basin (Nuccio and Condon, 1996).

Studied Salt Structures

Three principal salt structures are analyzed in this study: (1) the Cane Creek anticline, (2) the Moab Valley salt wall, and (3) the Big Bend minibasin. All three were active during Chinle deposition (Blakey and Gubitosa, 1984; Doelling, 1988; Hazel, 1994; Matthews et al., 2004) and have extensive exposure of Chinle Formation outcrops along their flanks.

The Cane Creek anticline is a salt-cored anticline (Figures 1B, 2). The Paradox salt thickens from 500 to about 1500 m (1600 to about 5000 ft) (Figure 2) within the core of the anticline (Joesling et al., 1966; Doelling and Chidsey, 2000). The fold trends northwest, parallel to the axis of the basin, and extends for roughly 50 km (31 mi) from the Green River in the northwest to the head of Kane Springs Canyon in the southeast (Figure 1B). The salt structure defines a buried pillow that has not breached any of the overlying stratigraphy (Figure 2). Chinle Formation strata crop out principally on the northeast flank of the anticline, extending from its crest to approximately 3 km (1.8 mi) downflank (Figure 1B).

The Moab Valley salt wall is approximately 20 km (12 mi) long and 3–4 km (1.8–2.4 mi) wide, trending northwest (Figure 1B). Paradox Formation salt occurs as cap rock along the present-day valley floor. In cross section, the salt forms a steep, vertical to overhanging wall, as constrained by well and seismic data within the valley (Trudgill et al., 2004) (Figure 2). The Chinle Formation directly abuts the salt on the southwestern flank of the structure, where upper Pennsylvanian to Lower Triassic strata (Honaker Trail, Cutler, and Moenkopi formations) are absent (Figure 2). Permian–Triassic strata also thin onto the northeastern flank of the salt wall (Trudgill et al., 2004), although postdepositional faulting obscures the details of this relationship. The exposed salt wall passes into a submerged salt-cored anticline at its northwestern end. This anticline was later exploited by the Moab fault, which exposes the Triassic outcrop on its southwestern flank (Trudgill et al., 2004). The Moab Valley salt wall is interpreted to have been a salt wall maintained by passive diapirism that formed a paleotopographic high during the Permian–Triassic (Matthews et al., 2004; Trudgill et al., 2004; Banbury, 2005). Chinle Formation strata are well exposed along the northwestern flank of the salt wall and follow the subsurface anticline extension of the structure for 15 km (9 mi) to the northwest (Figure 1B).

The Big Bend salt-withdrawal minibasin (Matthews et al., 2004) is approximately 6 × 6 km (3.6 × 3.6 mi)

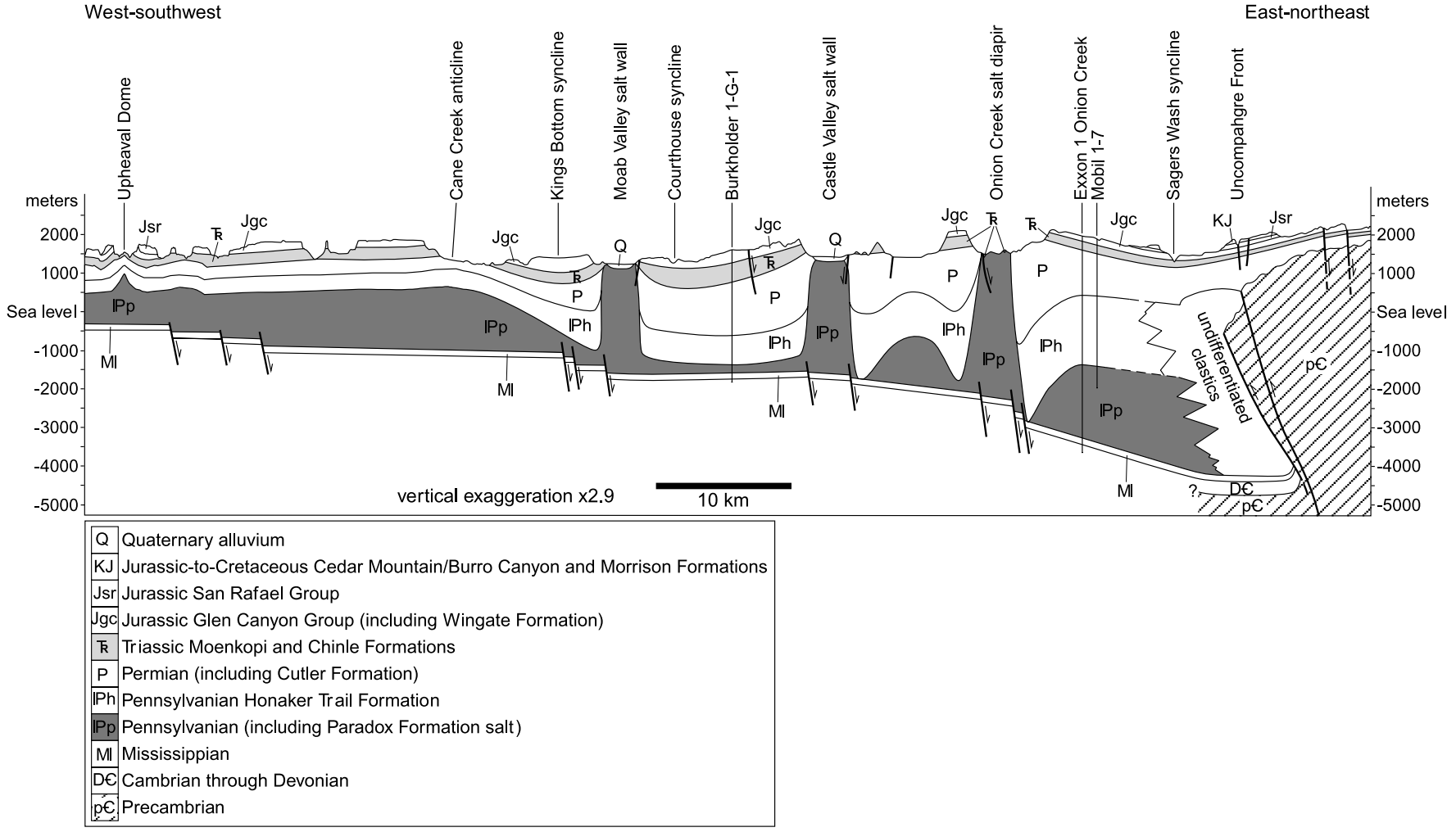

Figure 2. Regional cross section across the northeastern Paradox Basin showing present-day stratal architecture across major salt structures (modified from Trudgill et al., 2004; reproduced with the permission of the Gulf Coast Section SEPM Foundation). The line of cross section is located in Figure 1A.

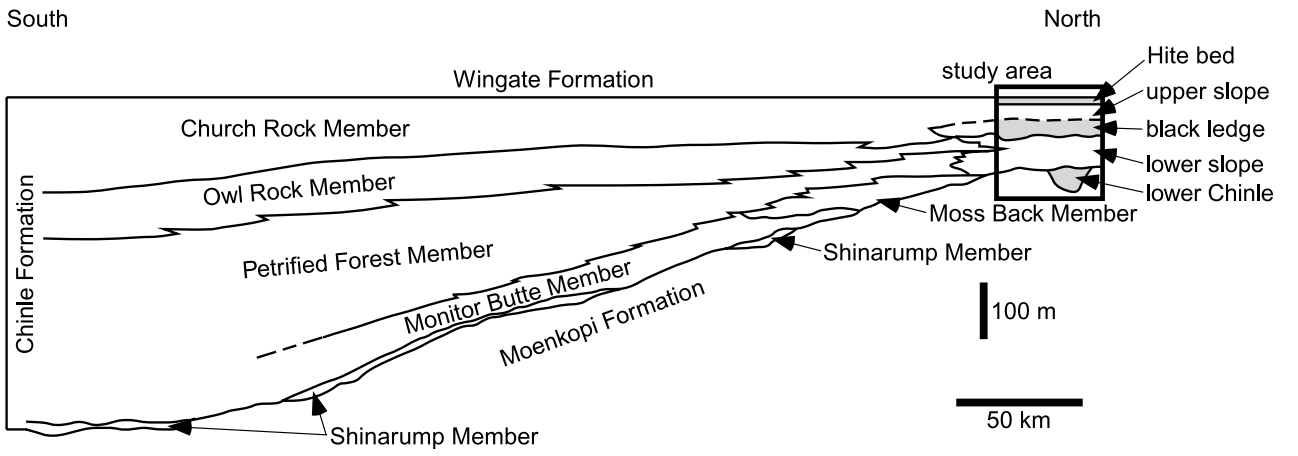

Figure 3. Generalized north-south cross section showing the regional lithostratigraphy of the Chinle Formation on the Colorado Plateau (after Blakey and Gubitosa, 1984; Hazel, 1994; Matthews et al., 2004; reproduced with the permission of the Gulf Coast Section SEPM Foundation) and its relationship to the informal local lithostratigraphy used in this article (within the box highlighting the study area). The line of cross section is located in Figure 1A.

in area and lies just to the south of a prominent kink in the Salt Valley-Cache Valley salt wall and to the northwest of the Castle Valley salt wall (Figure 1B). The surrounding salt walls were characterized by passive growth during the Permian–Triassic, including during Chinle Formation deposition (Matthews et al., 2004; Trudgill et al., 2004; Banbury, 2005).

Basin-Fill Stratigraphy

The general stratigraphy in the northeastern Paradox Basin has been described by many previous authors (e.g., Doelling, 1988, 2001), and its relationship to salt movement is interpreted by Trudgill et al. (2004). During the main period of salt movement (late Pennsylvanian to Triassic), deposition in the northeastern Paradox Basin was strongly controlled by salt tectonics (Doelling, 1988; Trudgill et al., 2004), resulting in a stratigraphy that contains abrupt lateral and vertical thickness changes. The effects of salt movement are most significant within the Pennsylvanian Honaker Trail and Permian Cutler formations, which display large thickness variations throughout the area (Figure 2). The effects of salt movement are less pronounced in Jurassic and Cretaceous strata overlying the Chinle Formation (Doelling, 1988; Trudgill et al., 2004).

Chinle Formation Regional Stratigraphy and Depositional Controls

The Chinle Formation is well documented across much of the southwestern United States, including the Colorado Plateau (e.g., Stewart et al., 1972; Blakey and Gubitosa, 1984; Dubiel, 1987; Lucas et al., 1997). Stewart et al. (1972) define six formal lithostratigraphic members within the formation, in ascending order: the Shinarump, Monitor Butte, Moss Back, Petrified Forest, Owl Rock, and Church Rock members (Figure 3) (see Lucas, 1993, for the proposed revision of the Chinle lithostratigraphy). This widely used lithostratigraphic subdivision of the Chinle Formation breaks down around the salt structures of the northeastern Paradox Basin (Figure 3) (Blakey and Gubitosa, 1984; Hazel, 1991, 1994). The Chinle Formation overlies the Middle Triassic Moenkopi Formation across a regional unconformity representing about 17 m.y. and associated locally with deep paleovalleys, which are infilled by the Shinarump Member (Stewart et al., 1972; Doelling, 2000). Over much of its extent, the top of the Chinle Formation is an unconformity, representing up to 15 m.y., with the overlying Lower Jurassic Wingate Sandstone (Stewart et al., 1972; Doelling, 2000). However, paleontologic data suggest that the Chinle-Wingate boundary may be locally conformable in the northeastern Paradox Basin (Lucas et al., 1997).

The lithostratigraphy of the Chinle Formation has been related to variations in facies architecture, driven by changes in regional accommodation (Blakey and Gubitosa, 1984; Lucas, 1993; Lucas et al., 1997). Extensive sheets of braided fluvial sandstones and conglomerates (e.g., Shinarump and Moss Back members) correspond to times of low regional accommodation and are interpreted to have regional, biostratigraphically distinctive unconformities at their bases (Lucas, 1993; Lucas et al., 1997). Widespread lacustrine mudstones with isolated fluvial sandstones (e.g., Monitor Butte, Petrified Forest,

Owl Rock, and Church Rock members) correspond to times of high regional accommodation. Maximum lake extent is recorded by freshwater limestone beds (Owl Rock Member). Changes in regional accommodation most likely reflect differences in the rate of regional tectonic subsidence (Blakey and Gubitosa, 1984). Coeval shallow-marine strata exhibit equivalent variations in facies architecture (Lucas and Marzolf, 1993; Lucas et al., 1997), consistent with regional tectonic subsidence and/or eustatic controls on relative sea level.

Regional climate during the deposition of the Chinle Formation is interpreted to have been subtropical monsoonal (Dubiel, 1987; Dubiel et al., 1991), although paleosol data imply semiarid conditions during some intervals (Prochnow et al., 2006a). The climate was sufficiently wet to sustain perennial fluviolacustrine depositional systems (Blakey and Gubitosa, 1984). Although climatic cycles may have driven features of the stratigraphic architecture (e.g., paleosol character; Prochnow et al., 2006a), the only strong trend is for increased aridity during deposition of the upper part of the Church Rock Member, which contains prominent desiccation features and small eolian deposits (Blakey and Gubitosa, 1984; Dubiel et al., 1991). Regional sediment sources for the formation are the Mogollan highlands in southern Arizona and northern New Mexico plus the Uncompahgre uplift and Front Range highlands in Colorado (Stewart, 1969; Dubiel, 1987).

DATA SET AND METHODS

The observations and interpretations presented in this article are based on detailed analysis of outcrop data. Sixteen measured sections have been logged over the study area (Figure 1B), and quantitative architectural data and paleocurrent readings were taken both at the logged sections and all other accessible outcrops. Additional thickness data have been collected from inaccessible outcrops (e.g., sheer cliff faces) using a laser rangefinder. High-resolution photomontages have been used, combined with all other outcrop data, to create facies panels for key locations.

Most of the measured sections were taken along a general transect of the area from southwest to northeast, following the line of the Colorado River as it cuts across various salt structures in the basin (Figure 1B). Some additional sections have been measured away from this line to gain a better three-dimensional understanding of selected relationships.

Outcrop gamma-ray logs were taken from three of the measured sections (numbered 2, 5, and 12 in Figure 1B) to link surface observations to nearby subsurface well data. The outcrop gamma-ray logs were collected with an EDA Instruments GRS-500 differential gamma-ray spectrometer. Wire-line-log data and lithological descriptions from 87 subsurface wells of variable quality and vintage (drilled between 1929 and 1993) have also been studied to interpret lithostratigraphic unit thicknesses across the region. These data were integrated with published outcrop and subsurface data (Doelling, 1988, 2001, 2002; Doelling and Ross, 1998; Doelling et al., 2002).

FACIES CHARACTER AND DEPOSITIONAL ENVIRONMENTS

The Chinle Formation contains seven facies associations, which are described and interpreted briefly below and summarized in Table 1. Facies associations are identified based on lithology, sedimentary structures, geometry, and nature of bedding contacts with underlying and overlying units. Intensity of bioturbation is described using the bioturbation index (BI) scheme of Taylor and Goldring (1993).

Facies Association 1: Fluvial Channel-Fill Sandstones

Description

This facies association comprises predominantly medium- to coarse-grained sandstones and gravel conglomerates, with subordinate fine-grained sandstones, arranged within erosively based channels (Figure 4A, B; Table 1). Channel-fill sandstones occur as isolated, single-story bodies and amalgamated, multistory, multilateral sheets, both of which are associated with overbank and channel-fill mudstones (facies association 2, Table 1).

Most isolated, single-story channel-fill sandstones are narrow (10–100 m; 33–330 ft) and shallow (2–5 m; 6.6–16 ft) with a low width/depth ratio (5:1–20:1; Hazel, 1994) and low-relief channel margins (Figure 4A). Channel bases are typically lined by mudclast lags. Medium- to coarse-grained sandstones are trough cross-bedded. Fine-grained sandstones, which preferentially occur near channel-fill margins, contain climbing current ripples. Channel margins are typically overlain by packages of inclined beds, with cross-bed paleocurrents aligned along the strike of the inclined

Table 1. Summary Sedimentology of Facies Associations in the Chinle Formation, Northeastern Paradox Basin*

Facies Associations	Lithology and Sedimentary Structures	Sand-Body Geometry	Sandstone Content (%)
1. Fluvial-channel-fill sandstones	Fine-, medium-, and coarse-grained sandstones and gravel conglomerates. Individual channels have basal lags and contain trough and tabular cross-beds, planar-parallel lamination, and climbing current ripples. (1) Isolated, single-story bodies are characterized by lateral accretion packages and represent meandering fluvial channels. (2) Multistory, multilateral sheets comprise amalgamated channels characterized by downstream accretion packages and represent braided fluvial channels.	(1) Isolated, single-story bodies: 10–100 m (33–330 ft) wide, 2–5 m (6.6–16.4 ft) thick. (2) Multistory, multilateral sheets: >100 m (>330 ft) wide, 10–30 m (33–100 ft) thick.	85–95
2. Fluvial overbank and channel-fill mudstones	Interbedded claystones, siltstones, and fine-grained sandstones. Laterally extensive successions contain thin, sharp-based, planar-parallel-laminated, and/or current-rippled sandstone sheets interpreted as fluvial-overbank flood deposits. Root traces, soil-indicative trace fossils, and mud cracks occur throughout sporadically. Laterally restricted successions occupy channelized scours, contain lateral accretion and drape packages, and are interpreted as fluvial channel-abandonment deposits.	Sandstone sheets: >100 m (>330 ft) wide and 1–200 cm (0.4–78 in.) thick	20–30
3. Lacustrine mudstones	Interbedded claystones, siltstones, and fine-grained sandstones with a high calcium carbonate content. Sandstones occur in thin, sharp-based, current-rippled, and/or parallel-laminated sheets interpreted as distal fluvial-overbank flood deposits. Roots are absent, and insect-larvae burrows occur at sandstone-bed tops, indicating subaqueous deposition.	Sandstone sheets: >100 m (>330 ft) wide, 1–50 cm (0.4–20 in.) thick	10–20
4. Moderately to completely bioturbated sandstones and mudstones	A wide range of grain sizes, reflecting a primary architecture comprising facies associations 1 and 2 (above). Moderate to complete bioturbation modifies the primary architecture. *Camborygma* (crayfish dwelling burrows) dominate, with subordinate root traces and pedogenic mottling, which indicates slow accumulation in flood-plain and/or marginal-lacustrine environments.	Where preserved, sand body geometry is comparable to facies associations 1 and 2	10–80
5. Paleosols	Claystones and siltstones, with subordinate poorly sorted sandstones and gravels. Abundant root traces, discoloration haloes, mottling, and calcareous rhizocretions. Subordinate soil-indicative trace fossils, mud cracks, and ferric concretions.	Sand bodies absent	10–20
6. Eolian sandstones	Well-sorted, well-rounded, fine- to medium-grained sandstones with subordinate claystones and siltstones. Sandstones contain high-angle cross-beds with alternating fine- and medium-grained laminae and represent eolian dune deposits. Claystones and siltstones containing mud cracks and scarce root traces represent interdune deposits.	Sandstone sheets: >1000 m (>3300 ft) wide and 0.5–5 m (1.6–16 ft) thick.	85–95
7. Disrupted beds	Deposits of facies associations 1–6 that have undergone localized, syn- or early postdepositional folding, faulting, and/or fracturing.	Highly variable	Highly variable

*See text for discussion of key features in each facies association.

beds. These inclined beds record lateral accretion of channel margins.

Amalgamated, multistory, multilateral sheet sandstones are thick (10–30 m; 33–100 ft), with a high width/depth ratio (>100:1; Hazel, 1994). Where individual channel stories can be distinguished, they have basal lags containing mudclasts, silicified wood, and angular sandstone intraclasts. Packages of inclined beds 1–5 m (3.3–16 ft) thick and 10–50 m (33–164 ft) in dip extent commonly overlie channel bases and other prominent erosion surfaces (Figure 4B). Most trough and tabular cross-sets and climbing current ripples have paleocurrents aligned down the dip of the inclined beds, recording downstream accretion of the inclined surface, although some packages of inclined beds record lateral accretion (Figure 4B) (Hazel, 1991, 1994). Planar-parallel laminated beds containing parting lineations also occur, indicating upper-flow-regime conditions in some beds. Localized soft-sediment folding, dewatering pipes and load structures, and structureless beds are common in fine-grained sandstones.

Interpretation

Facies association 1 is interpreted to represent the deposits of various sandy fluvial systems. Isolated, single-story channel-fill sandstones are interpreted as meandering river deposits, based on (1) their association with lateral accretion deposits, which represent point-bar migration; (2) their isolated character within surrounding overbank mudstones; and (3) their low width/depth ratios (Dubiel, 1987; Hazel, 1991, 1994). Mudclast lags record erosion and reworking of adjacent overbank mudstones, whereas the abundance of trough cross-bedded sandstones indicates consistent, moderate flow velocities. Climbing current ripples indicate episodes of rapid deposition, possibly during the waning stages of episodic floods.

Amalgamated, multistory, multilateral sheet sandstones are interpreted as braided-river deposits, based on (1) the occurrence of multiple, stacked channels; (2) their association with downstream-accretion deposits, which most likely represent midchannel bar migration; and (3) their high width/depth ratios (Hazel, 1991, 1994). The abundance of downstream-accretion and lateral-accretion deposits, which imply the common occurrence of midchannel and side-attached bars, are typical of deep, perennial, sandy braided rivers (Cant and Walker, 1978; Miall, 1978). The mixed composition of channel-base lags records a greater extent or degree of erosion than do mudclast lags at the base of isolated channels. These lags, combined with the occurrence of structures that record variable flow velocities, provide evidence of fluctuating, and possibly flashy, discharge (Hazel, 1991, 1994). Localized soft-sediment deformation is attributed to liquefaction and/or slumping, which are commonly associated with bank collapse, flood flows, and rapid sedimentation in fluvial systems (e.g., Martin and Turner, 1998).

Facies Association 2: Fluvial Overbank and Channel-Fill Mudstones

Description

This facies association consists predominantly of parallel-laminated claystones and siltstones, with subordinate micaceous, fine-grained sandstones (Figure 4A; Table 1). Interbedded claystones, siltstones, and fine-grained sandstones occur as laterally extensive successions that are eroded into by channel-fill sandstones (facies association 1, Table 1) or as laterally restricted successions within channelized scours that are associated with channel-fill sandstones (facies association 1, Table 1). The latter is associated with inclined beds that drape one margin of the channelized scour at angles up to 30°. Fine-grained sandstones typically occur as thin (1–10-cm [0.4–4-in.]-thick), sharp-based beds containing planar-parallel lamination and/or current ripples, but some occur in climbing-current-rippled beds up to 2 m (6.6 ft) thick. Most interbedded successions of claystones, siltstones, and fine-grained sandstones exhibit fining-upward cycles of 5–50 cm (2–20 in.) thickness. Sparse root traces and/or mud cracks are seen at the top of some cycles. Bioturbation is absent to low in intensity (BI of 0–2), and common trace fossils include horizontal burrows attributable to soil-dwelling insects and beetles (Hasiotis, 2002).

Interpretation

The dominantly fine-grained and parallel-laminated character of the deposits in facies association 2 implies deposition from suspension in a low-energy environment. Planar-parallel-laminated and current-rippled sandstone beds indicate rapid episodes of sand deposition from high-velocity unidirectional flows. Where such beds occur in laterally extensive successions, their facies context suggests that they most likely represent splays or sheets associated with overbank flooding of nearby fluvial-channel-fill sandstones (facies association 1). Fining-upward cycles in these successions record episodes of overbank deposition on a river flood plain, and the occurrence of root traces and/or mud cracks

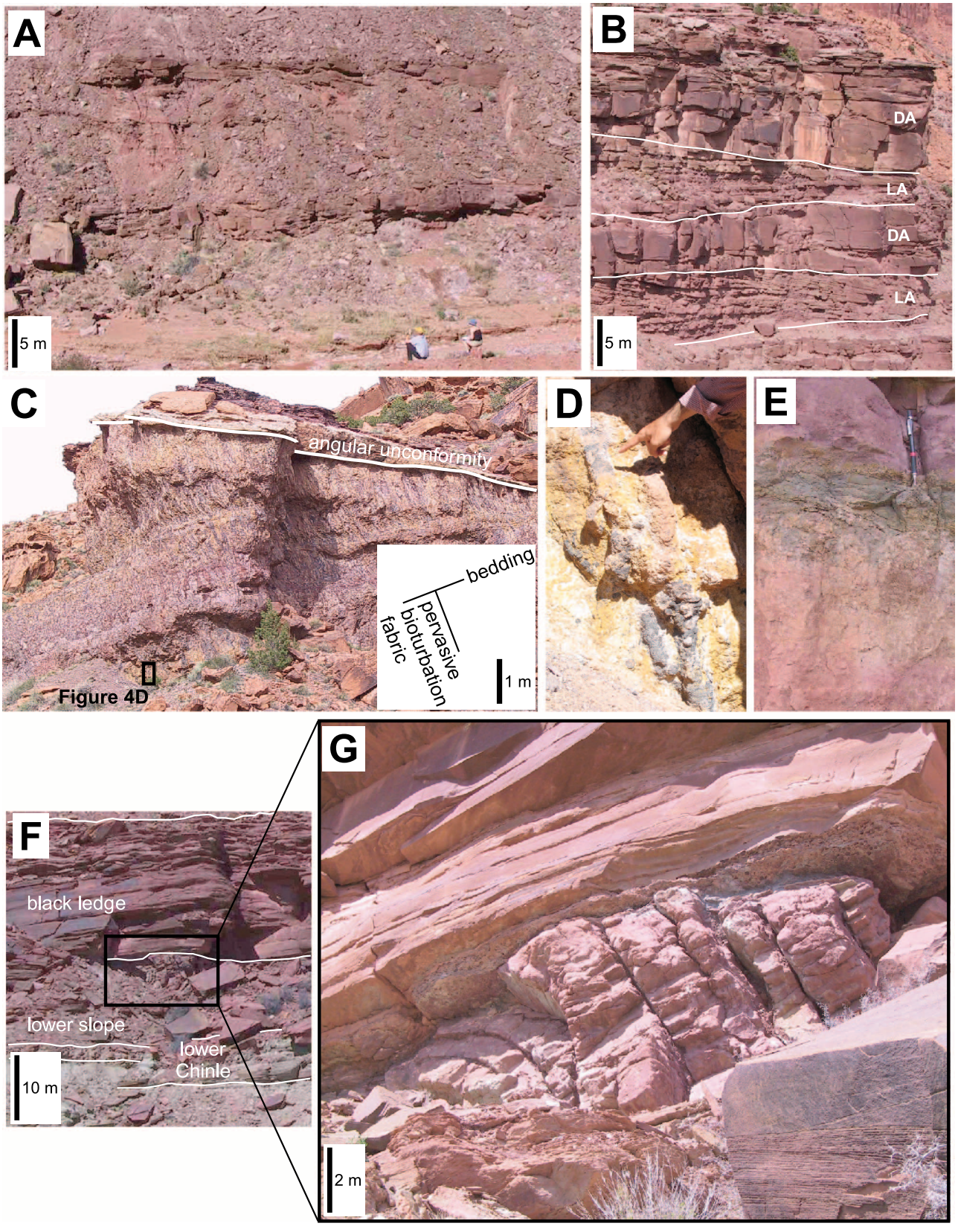
A
5 m
B
DA
LA
DA
LA
5 m
C
angular unconformity
bedding
pervasive bioturbation fabric
1 m
Figure 4D
D
E
F
black ledge
lower slope
lower Chinle
10 m
G
2 m

record repeated subaerial exposure and desiccation. Soil-dwelling insect and beetle traces suggest non-waterlogged conditions with soil moisture levels of 7–37% (Hasiotis, 2002). Laterally restricted successions within channelized scours most likely represent fluvial-channel-abandonment deposits. The occurrence of inclined lateral-accretion and drape deposits within these successions suggest that the fluvial systems were meandering.

Facies Association 3: Lacustrine Mudstones

Description

Facies association 3 is composed predominantly of claystones and siltstones occurring in finely parallel-laminated successions up to 50 m (164 ft) thick (Table 1). Subordinate fine-grained sandstones occur in laterally extensive (up to several kilometers) beds up to 50 cm (20 in.) thick, containing parallel lamination and/or current ripples. Both mudstones and sandstones have a high calcium carbonate content, and rare, thin (<1-m; <3.3-ft) limestone beds and stringers are present. Bed tops exhibit a low intensity of bioturbation (BI of 1–2) by horizontal burrows attributable to insect larvae (*Fuersichnus*; Hasiotis, 2002). A distinct absence of roots is observed within these deposits, and they are only rarely associated with channel-fill sandstones or mudstones (facies association 1, Table 1). However, deposits of facies association 3 commonly pass gradationally into overbank mudstones (facies association 2, Table 1), both vertically and laterally.

Interpretation

The absence of roots and occurrence of insect-larvae burrows imply that the fine-grained, finely laminated deposits of facies association 3 were deposited from suspension in shallow water (e.g., Hasiotis, 2002). Given their facies context, laterally adjacent to fluvial-overbank deposits (facies association 2, Table 1), these deposits are attributed to shallow perennial lakes. Fine-grained sandstone sheet beds are interpreted to be fluvially derived, and their similarity to overbank splay and sheet sandstones (in facies association 2, Table 1) suggests that they most likely record distal overbank floods. Siliciclastic claystones and siltstones are also interpreted to be fluvially derived. The high calcium carbonate content is interpreted to record inorganic calcium carbonate precipitation, with limestone beds recording periods of reduced siliciclastic-sediment supply (e.g., Talbot and Allen, 1996), although some early diagenetic effects are evident in limestone bed and stringer geometries.

Facies Association 4: Moderately to Completely Bioturbated Sandstones and Mudstones

Description

Most of the facies associations within the Chinle Formation are bioturbated to a small degree (BI of 1–2), but this facies association comprises moderately to completely bioturbated deposits (BI of 3–6). Individual burrows are commonly only poorly resolved, and the association is characterized by a pervasive fabric that (1) partially or completely destroys the primary bedding and (2) is approximately perpendicular to primary bedding (Figure 4C, D; Table 1). Bioturbation intensity varies between packages of beds in a vertical succession. The dominant trace fossils are crayfish dwelling burrows (*Camborygma*; Hasiotis and Mitchell, 1989; Hasiotis et al., 1993; Hasiotis, 2002), which form subvertical tubes 5–20 cm (2–8 in.) in diameter and up to 2 m (6.6 ft) long. Subordinate root traces and pedogenic mottling are also present, but do not dominate the fabric (unlike in facies association 5, Table 1). Where preserved (i.e., in bedding-concordant packages

Figure 4. Photographs illustrating the character of selected facies associations (Table 1). (A) Isolated channel-fill sandstones (facies association 1) surrounded by overbank mudstones (facies association 2) (lower-slope unit, lower Long Canyon measured section, numbered 3 in Figure 1B). (B) Multistory channel-fill sandstones (facies association 1) containing both downstream-accretion (DA) and lateral-accretion (LA) packages (black-ledge unit, upper Long Canyon measured section, numbered 2 in Figure 1B). (C, D) Moderately to completely bioturbated sandstones and mudstones (facies association 4) exhibiting a pervasive fabric produced by crayfish burrows (*Camborygma*) (lower Chinle unit, Big Bend minibasin, Figure 1B) (from Matthews et al., 2004; reproduced with the permission of the Gulf Coast Section SEPM Foundation). The burrows were originally subvertical (Hasiotis, 2002), but have subsequently been rotated with bedding. (E) Weakly developed paleosol (facies association 5) (upper-slope unit, Jackass Canyon measured section, numbered 8 in Figure 1B). (F, G) Folded, overturned sandstones and siltstones (facies association 7) truncated by the subregional unconformity at the base of the black-ledge unit (uppermost lower-slope unit, Sevenmile Canyon measured section, numbered 16 in Figure 1B).

with BI of 3), the primary depositional fabric contains coarse- to very coarse-grained, channel-fill sandstones of variable stacking density in a matrix of mudstones and rare sheet sandstones. This preserved primary fabric strongly resembles that of facies associations 1 and 2 (Table 1). Where the primary fabric is largely destroyed (i.e., in bedding-concordant packages with BI of 4–6), the association consists of poorly to very poorly sorted sandy siltstones, silty sandstones, and silty gravels.

Interpretation

Interpretations of this association are based largely on the abundance of crayfish dwelling burrows, which indicates deposition in poorly drained subaerial environments with a high (1–2 m [3.3–6.6 ft] below the surface) and fluctuating water table (Hasiotis, 2002). The occurrence of subordinate roots and pedogenic mottling is consistent with such a setting, as is the primary bedding architecture of fluvial-channel-fill sandstones and overbank mudstones (facies associations 1 and 2, respectively, Table 1). Abundant crayfish occur in humid to hot, wet seasonal climates (Hasiotis, 2002). The intensity of bioturbation reflects the rate of sedimentation, with more intensely bioturbated packages having accumulated more slowly. The association is interpreted to represent flood-plain and/or marginal-lacustrine environments that accumulated under low sedimentation rates.

Facies Association 5: Paleosols

Description

This facies association comprises predominantly claystones and siltstones, with subordinate poorly sorted sandstones and gravels. The association occurs as thin (10–200-cm; 4–78-in.) bedding-concordant intervals characterized by abundant root traces with associated discoloration haloes, mottling, and calcareous rhizocretions (Figure 4E, Table 1). Subordinate burrows also occur, including crayfish dwelling burrows (cf. facies association 4, Table 1) and burrows attributable to soil-dwelling insects (Hasiotis, 2002). Sand-filled mud cracks and ferric concretions are present locally. In contrast to overbank and channel-fill mudstones (facies association 2, Table 1), primary bedding is largely to completely destroyed by root traces and other pedogenic structures. The intensity of bedding-fabric destruction, color, and relative proportions of different pedogenic structures varies between different units of facies association 5 and also between beds in thick successions of the association (e.g., Prochnow et al., 2005, 2006b).

Interpretation

The abundance of root traces and associated pedogenic structures indicates that deposits of facies association 5 represent paleosols. The occurrence of mud cracks suggests episodic drying and desiccation, whereas soil-dwelling traces suggest moderate soil moisture content (7–37%; Hasiotis, 2002). In combination, these features suggest a fluctuating water table consistent with a regional subtropical, monsoon-seasonal climate (Dubiel, 1987; Dubiel et al., 1991). The presence of calcareous rhizocretions and ferric concretions also supports this climatic interpretation (Retallack, 2001). Variations in the intensity of bedding-fabric destruction, color, and relative proportions of different pedogenic structures between paleosols are interpreted to reflect differing degrees of development, related to the duration and/or paleogeographic location of soil formation (e.g., Kraus, 1997; Retallack, 2001; Prochnow et al., 2005, 2006b). Such variations within thick vertical successions record the formation of different soil horizons within well-developed paleosols and/or the vertical stacking of paleosols at different stages of development. All the studied paleosols mark a depositional hiatus. More detailed analyses of pedogenic structures and paleosols in the Chinle Formation are presented by Dubiel (1987), Hasiotis and Dubiel (1994), Hasiotis (2002), and Prochnow et al. (2005, 2006b).

Facies Association 6: Eolian Sandstones

Description

Facies association 6 consists predominantly of well-sorted and well-rounded, fine- to medium-grained sandstones that typically occur in laterally extensive (>1-km; >0.6-mi) sheets of 0.5–5 m (1.6–16.4 ft) thickness (Table 1). Sandstone sheets are sharp based with minor (<10-cm; <4-in.) erosional relief at their base. The sheets contain stacked, high-angle trough and tabular cross-beds in which successive foreset laminae exhibit alternations in grain size from fine- to medium-grained sandstone. Sheets are separated by thin (<10-cm; <4-in.) claystone and siltstone intervals that contain sand-filled mud cracks and scarce root traces.

Interpretation

Sandstone sheets are interpreted as the deposits of migrating eolian dunes, based on (1) the well-sorted and well-rounded character of sandstone grains, (2) the high angle of cross-bed sets, and (3) the alternating fine- and medium-grained character of the foresets, which record grainfall and grainflow processes (e.g., Kocurek, 1996).

Claystone and siltstone intervals separating the sandstone sheets are interpreted as wet interdune deposits (e.g., Ahlbrandt and Fryberger, 1981; Glennie, 1987; Thomas, 1997).

Facies Association 7: Disrupted Beds

Description

All of the facies associations described above are locally disrupted by folding, faulting, and/or fracturing in a manner that is not inherent to any particular association. These various disrupted beds comprise facies association 7 (Figure 4F, G; Table 1). Flat-lying beds erosively truncate underlying folds, faults, and fracture sets of the facies association. Folded units are 2–15 m (6.6–49 ft) thick and 10–400 m (33–1312 ft) wide and pass laterally into undisturbed deposits. Folds are typically asymmetric, with one limb dipping at, or close to, regional tectonic dip, and the other limb with near-vertical or overturned dips. Faults typically have small offsets (<1 m; <3.3 ft). Primary sedimentary structures such as rippled surfaces, cross-bedding, and desiccation cracks are well preserved in folded units and can be used to deduce younging directions and, in some instances, provide evidence that the beds were originally paleohorizontal. Selected structures are described and interpreted in more detail below.

Interpretation

This facies association comprises units that have undergone ductile and/or brittle deformation. The limited lateral extent of the deformation implies a localized driving mechanism, whereas the truncation of folds, faults, and fracture sets by flat-lying beds indicates that deformation occurred during or soon after deposition. Fold asymmetry suggests a sense of movement, most likely because of slumping down a paleoslope (Matthews et al., 2004). The non-facies-association-specific character of the deformation implies a tectonic mechanism that was not restricted to a particular environment.

SUBREGIONAL STRATIGRAPHY

The regional lithostratigraphy of the Chinle Formation is not readily applicable to the northeastern Paradox Basin (Blakey and Gubitosa, 1984; Hazel, 1991, 1994) (Figure 3). Instead, the lithostratigraphic terminology of Hazel (1991, 1994) is adapted to subdivide the formation into five informal lithostratigraphic units that can be mapped throughout much of the northeastern Paradox Basin: in ascending order, the lower Chinle, lower-slope, black-ledge, upper-slope, and Hite bed units (Matthews et al., 2004) (Figures 3, 5). The diagnostic facies character, stratigraphic boundaries, and gamma-ray-log response of these five units are illustrated in a type outcrop section (from Long Canyon, numbered 2 in Figures 1B, 5A) and subsurface gamma-ray log (Shell Oil 2 Gruvers Mesa well, labeled in Figures 1B, 5B).

The Lower Chinle Unit

The lower Chinle unit ranges from 0 to more than 50 m (164 ft) in thickness across the study area and is bounded by a regional angular unconformity with the Moenkopi Formation below (Stewart et al., 1972) and a distinct change in facies character and a local angular unconformity with the lower-slope unit above (Figure 5) (Doelling and Ross, 1998). Dominant facies associations are isolated and multistory channel-fill sandstones, bioturbated sandstone and mudstones, and paleosols (facies associations 1, 4, and 5; Table 1). Channel-fill sandstones are quartz rich and pebbly, with a distinctive white color (''basal sandstone unit'' of Stewart et al., 1972; ''white grit'' of Matthews et al., 2004). Pebbles and subangular clasts of quartz, chert, and limestone occur in channel lags and are interpreted to be derived from upper Paleozoic chert-bearing limestones eroded from the Uncompahgre uplift (Hazel, 1994). Paleosols and intensely bioturbated deposits are strongly color mottled (''mottled strata'' of Stewart et al., 1972; Hazel, 1994; Matthews et al., 2004). The unit has a high sandstone content (70–100%), and its gamma-ray-log character is generally low because of its clean, quartz-rich petrography (Figure 5B). Distinctive high gamma-ray spikes are present, reflecting concentrations of uranium (Figure 5B) (Stewart et al., 1959). The lower Chinle unit is most likely time and facies equivalent to the regional Moss Back Member (Figure 3) (Stewart et al., 1959; Hazel, 1991, 1994) and, based on paleoclimate reconstructions, the lower part of the Petrified Forest Member (Prochnow et al., 2006a). However, it may also correspond locally to older units, including the Shinarump Member (Lucas et al., 1997, p. 85).

The Lower-Slope Unit

The lower-slope unit is 15–80 m (49–262 ft) thick, overlies the lower Chinle unit across either a gradational contact or a local angular unconformity, and is truncated by a subregional erosional unconformity at

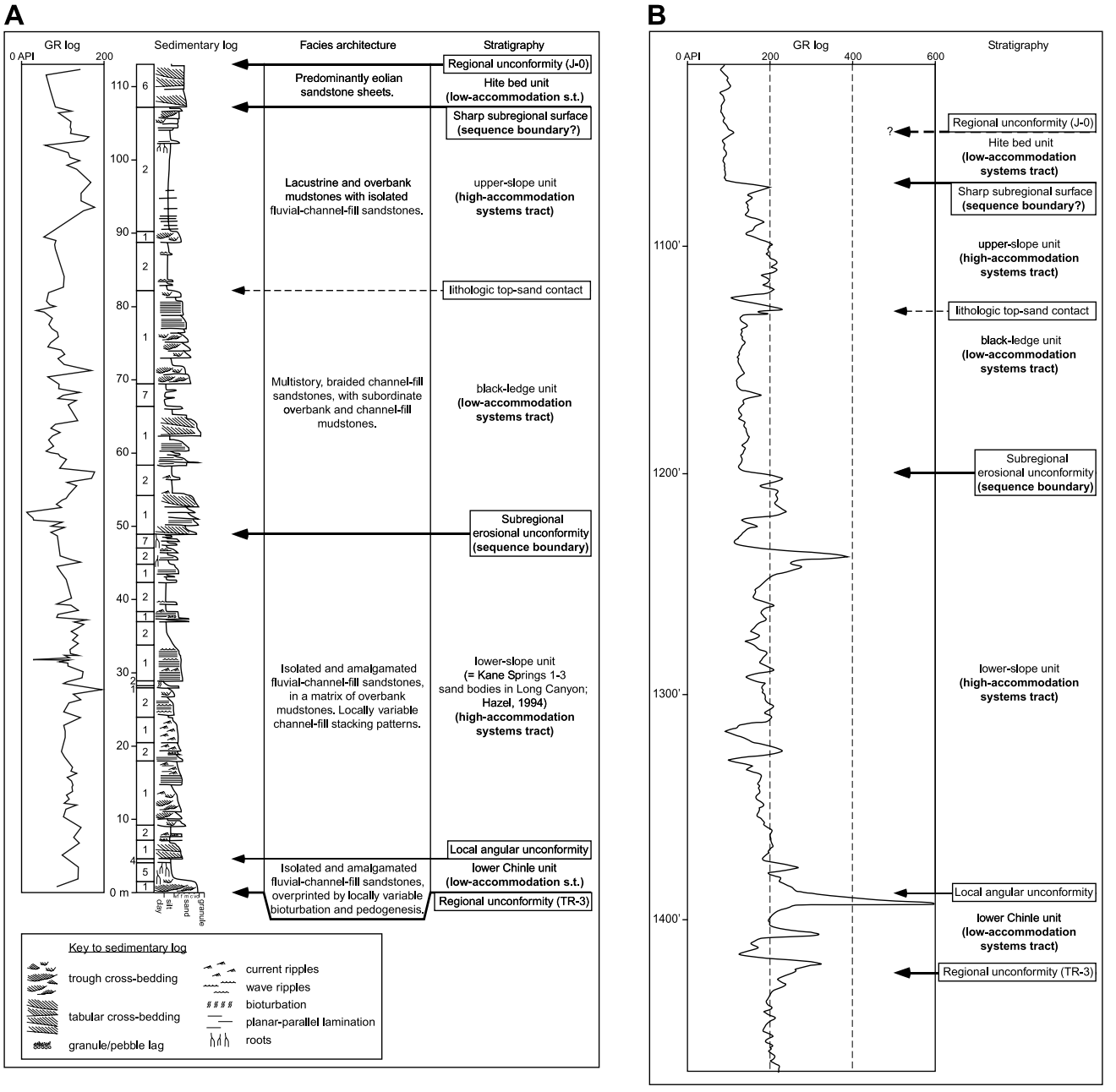

Figure 5. Type outcrop and subsurface successions through the Chinle Formation, illustrating its facies character and architecture, informal lithostratigraphy, sequence stratigraphy, and gamma-ray-log character. (A) Measured outcrop section and gamma-ray log through the upper part of Long Canyon (numbered 2 in Figure 1B). (B) Subsurface gamma-ray log from Shell Oil 2 Gruvers Mesa well (Figure 1B).

the base of the overlying black-ledge unit (Figure 5). Dominant facies associations are isolated channel-fill sandstones and overbank and channel-fill mudstones (facies associations 1, 2; Table 1), with subordinate paleosols and disrupted beds (facies associations 5, 7; Table 1). Disrupted beds are particularly common below the contact with the overlying black-ledge unit (e.g., Figure 5A). Stacking of channel-fill sand bodies is variable and locally defines stratigraphic units within the lower-slope unit (e.g., Kane Springs sand bodies 1–3 on the northeastern flank of the Cane Creek anticline, Figure 1B) (Hazel, 1991, 1994). However, these units cannot be traced across the study area and consequently have not been applied here. Hazel (1991, 1994)

also noted an uncommonly high proportion of locally derived, pedogenic-carbonate nodules reworked into channel-fill lags in the lower-slope unit in the Cane Creek anticline area (Figure 1B). The unit has a variable and moderate sandstone content (30–60%). Its gamma-ray-log character comprises (1) sharp-based units of low gamma-ray response, corresponding to channel-fill sandstones; (2) low gamma-ray spikes, representing overbank sandstone sheets; and (3) intervals of moderate to high, serrate gamma-ray response, corresponding to mudstone-dominated overbank deposits (Figure 5). On the basis of field mapping to the south and west of the study area, Gubitosa (1981) and Hazel (1991, 1994) interpret the lower-slope unit to be time correlative to parts of the regional Petrified Forest and Owl Rock members (Figure 3). Paleoclimate reconstructions support the correlation of the lower-slope unit to the upper Petrified Forest Member (Prochnow et al., 2006a). Alternatively, the lower-slope unit has been correlated to the Shinarump and Monitor Butte members (Lucas et al., 1997, p. 85).

The Black-Ledge Unit

The black-ledge unit is 3–70 m (10–229 ft) thick, with a subregional erosional unconformity at its base and gradational contact with the overlying upper-slope unit at its top. The basal unconformity is marked by (1) a discontinuous lag of intra- and extraformational clasts, including clasts of the underlying Moenkopi and Cutler formations; (2) local angular discordances in bedding; and (3) the localized(?) development of enhanced early cementation below the surface, prior to compaction (Miall and Arush, 2001, p. 977–978). The unit is composed predominantly of multistory, braided channel-fill sandstones (facies association 1; Table 1), with subordinate overbank and channel-fill mudstones, paleosols, and disrupted beds (facies associations 2, 5, 7; Table 1). The unit has a high sandstone content (80–100%), and its gamma-ray-log character is correspondingly low (Figure 5), with an abundance of sharp-based units of low gamma-ray response, corresponding to individual channel-fill sandstone stories. The black-ledge unit has been identified previously as a mappable unit over much of the northeastern Paradox Basin (e.g., Stewart et al., 1959) and most likely corresponds to the base and/or lower part of the regional Church Rock Member (Figure 3) (Blakey and Gubitosa, 1984; Hazel, 1991, 1994). The black-ledge unit has also been correlated to the Moss Back Member (Lucas et al., 1997, p. 85).

The Upper-Slope Unit

The upper-slope unit gradationally overlies the black-ledge unit, ranges between 10 and 75 m (33–246 ft) in thickness across the study area, and is overlain across a sharp surface by the Hite bed unit. Dominant facies associations are overbank and lacustrine mudstones (facies associations 2, 3; Table 1), punctuated by bioturbated and root-penetrated, calcareous thin beds. Isolated channel-fill sandstones and paleosols (facies associations 1, 5; Table 1) also occur. East of the Big Bend minibasin (Figure 1B), the unit becomes dominated by lacustrine mudstones, which are relatively carbonate rich. The sandstone content of the unit is generally low (20–30%), although localized clustering of channel-fill sandstones results in moderate values (50–60%; e.g., at Courthouse Wash measured section, numbered 5 in Figure 1B). The gamma-ray-log character of the upper-slope unit is similar to that of the lower-slope unit, consisting of an overall moderate to high gamma-ray response with sharp-based units and spikes of low gamma-ray response, corresponding to channel-fill sandstones and sandstone sheets, respectively (Figure 5). The upper-slope unit is time equivalent to part of the regional Church Rock Member (Figure 3; Blakey and Gubitosa, 1984; Hazel, 1991, 1994) or, alternatively, part of the Petrified Forest Member (Lucas et al., 1997, p. 85).

The Hite Bed Unit

The Hite bed unit is thin (0–12 m; 0–39 ft) and is bounded by a sharp surface with the underlying upper-slope unit and a regional angular unconformity with the Jurassic Wingate Sandstone above (Stewart et al., 1972). The dominant facies association is eolian sandstones (facies association 6; Table 1), although isolated channel-fill sandstones and overbank and channel-fill mudstones occur locally (facies associations 1, 2; Table 1). The unit is interpreted to contain both eolian and fluvially reworked eolian deposits, which record increased climatic aridity relative to the underlying upper-slope unit (Dubiel, 1987; Hazel, 1991). Lateral variations in the thickness of the Hite bed unit have been attributed to infilling of topographic lows (Dubiel, 1987). Sandstone content is very high (90–100%), and the unit has a uniform, low gamma-ray response with rare high gamma-ray spikes corresponding to interbedded mudstones (Figure 5). This gamma-ray character is very similar to that of the overlying Wingate Sandstone, and it is difficult to distinguish the two in

wire-line-log data (e.g., Figure 5B). The Hite bed unit corresponds in age to the uppermost Church Rock Member (Figure 3) (Blakey and Gubitosa, 1984; Hazel, 1991, 1994; Lucas et al., 1997, p. 85).

Sequence-Stratigraphic Framework

The stratigraphic boundaries and units described above (Figure 5) are used to construct a subregional sequence-stratigraphic framework for the Chinle Formation in the northeastern Paradox Basin. The sequence stratigraphy interpreted below is based on mapped geometric stratal relationships and changes in facies architecture, but it cannot be related to the regional biostratigraphy of the Chinle Formation (Lucas, 1997; Lucas et al., 1997) in the absence of comprehensive paleontologic data. The sequence stratigraphy of the Chinle Formation was not directly driven by relative changes in sea level, which had little effect within this depositional setting (e.g., Blakey and Gubitosa, 1984). Instead, we interpret stratigraphic architecture and associated systems tracts to reflect variations in the rate of accommodation generation. Poorly connected fluvial-channel-fill sandstones encased in overbank and lacustrine mudstones are interpreted to reflect deposition under high accommodation conditions and are assigned to high-accommodation systems tracts. Multistory channel-fill sandstones, well-developed paleosols, and intensely bioturbated intervals are interpreted to record slow rates of vertical aggradation in a low accommodation setting and are assigned to low-accommodation systems tracts.

The lower Chinle unit is bounded by underlying and overlying unconformities, of regional and local extent, respectively (Figure 5). The thin, discontinuous character of the lower Chinle unit itself and the abundance of paleosols and bioturbated sandstones and mudstones are used to assign the unit to a low-accommodation systems tract (Figure 5). In general, the overlying lower-slope unit contains a relatively low proportion of channel-fill sandstones, which are isolated, and a high proportion of preserved overbank and channel-fill mudstones. This facies architecture suggests the aggradation of predominantly meandering rivers and flood plains within a high-accommodation systems tract (Figure 5). The base of the black-ledge unit is marked by a subregional erosional unconformity, interpreted as a sequence boundary (sensu Van Wagoner et al., 1988) (Figure 5). The high proportion of braided fluvial-channel-fill sandstones and low proportion of preserved overbank and channel-fill mudstones in the black-ledge unit suggest aggradation of a braid plain(s) within a low-accommodation systems tract (Figure 5). The occurrence of an underlying sequence boundary is consistent with this interpretation. The overlying upper-slope unit is characterized by a high proportion of lacustrine and overbank mudstones and a relatively low proportion of isolated channel-fill sandstones. This facies architecture records the development of lakes and coeval aggradation of predominantly meandering rivers and flood plains within a high-accommodation systems tract (Figure 5). The base of the upper-slope unit is gradational with the underlying black-ledge unit, suggesting that there was a gradual increase in accommodation between the two units and their associated systems tracts. The base of the Hite bed unit is a sharp, subregional surface (Figure 5) marked by an increase in climatic aridity (Dubiel, 1987; Hazel, 1991). The thin character of the Hite bed, combined with the occurrence of multiple rooted and/or desiccated surfaces that record minor hiatuses within the unit, implies deposition within a low-accommodation systems tract. This interpretation implies that the base of the Hite bed is a sequence boundary (e.g., Lucas et al., 1997, p. 98–99), but features such as paleovalleys need to be identified outside of the study area to support this view.

The sequence-stratigraphic surfaces and the systems tracts that they bound have only been mapped inside the study area (about 5300 km^2 [2046 mi^2]), instead of over the entire depositional basin of the Chinle Formation (Figure 1A), and the resulting sequence-stratigraphic framework is provisional. Nevertheless, the subregional extent of the framework, across multiple growing salt structures, requires a subregional driving mechanism. The most likely mechanism is subregional tectonic subsidence, with higher subsidence rates corresponding to high-accommodation systems tracts (e.g., Blakey and Gubitosa, 1984). Additional, probable subregional influences are (1) hinterland climate and tectonics in the Uncompahgre uplift area, which influenced sediment flux into the basin (e.g., Dubiel, 1987); and (2) basin-flank morphology, which influenced both the volume of accommodation in the northeastern Paradox Basin and the surface area of the Uncompahgre uplift sediment source. The latter influence is illustrated by the transition from the black-ledge unit to the overlying upper-slope unit, which coincides with onlap of the central part of the Uncompahgre uplift basement at the northeastern flank of the basin and a corresponding increase in basin volume and decrease in surface area of the sediment source.

SALT-INFLUENCED SEDIMENTATION PATTERNS

Three indicators of salt-sediment interaction are analyzed subregionally and at a local scale across the studied salt structures: (1) stratigraphic thickness changes, (2) angular stratal relationships, and (3) internal facies architecture.

Stratigraphic Thickness Changes

A subregional, southwest-northeast cross section across the study area demonstrates that the stratigraphic thicknesses of informal lithostratigraphic units within the Chinle Formation vary across the Cane Creek anticline, Moab Valley salt wall, and Big Bend minibasin (Figure 6) (Matthews et al., 2004).

The lower Chinle unit displays the greatest degree of thickness variability. It is thin (<10 m; <33 ft) or absent over much of the northeastern Paradox Basin (Figures 6, 7A), but thickened sections occur locally in four areas: (1) the Big Bend minibasin (>50 m; >164 ft), (2) between the Moab Valley and Castle Valley salt walls (>30 m; >100 ft), (3) in isolated patches along the southwestern flank and crest of the present-day Cane Creek anticline (up to 20 m [66 ft]), and (4) in the northwestern corner of the study area (up to 35 m [115 ft]). The lower-slope unit is present as a broad northeast-trending belt of 20–50 m (66–164 ft) thickness across most of study area, and it thins away from this belt toward the southeast and northwest (Figures 6, 7B). Anomalously thick (>50-m; >164-ft) and thin (<20-m; <66-ft) sections occur locally: (1) in isolated patches along the crest of the present-day Cane Creek anticline, (2) northwest of the Moab Valley salt wall, and (3) in the west-central part of the study area. The black-ledge unit is generally 10–20 m (33–66 ft) thick, but thins and becomes less distinct to the east of the Big Bend minibasin (Figures 6, 7C). Anomalously thick (>30-m; >100-ft) sections occur locally (1) in an isolated patch along the crest of the present-day Cane Creek anticline, (2) along the southwestern flank of the Moab Valley salt wall, and (3) in the northwestern corner of the study area. The upper-slope unit is generally 20–40 m (66–131 ft) thick (Figures 6, 7D) and unconformably overlies the Uncompahgre uplift, which lies just outside the eastern boundary of the study area. Pronounced localized thickening of the unit occurs (1) in isolated patches along the southwestern flank and crest of the present-day Cane Creek anticline (up to 60 m [196 ft]), (2) along the flanks of the Moab Valley salt wall (up to 75 m [246 ft]), (3) along the flanks of the Salt Valley salt wall (>60 m; >196 ft), and (4) in the southwestern corner of the study area (up to 60 m [196 ft]). The Hite bed unit is 0–12 m (0–39 ft) thick at outcrop (Figure 6), but cannot be clearly distinguished from the overlying Wingate Sandstone in subsurface well logs (e.g., Figure 5B). Accordingly, no isopach map has been constructed for this unit.

Some of the thickness changes described above can be attributed to mechanisms other than syndepositional salt tectonics: (1) identification of lithostratigraphic units in subsurface well-log data is uncertain, (2) anomalous thicknesses in the subsurface may reflect omission or repetition of strata across faults, and (3) thickness variations may reflect lateral facies changes between time-equivalent lithostratigraphic units (e.g., across the gradational boundary between the black-ledge and upper-slope units; Figure 7C, D). Nevertheless, some recurring trends imply a halokinetic control on stratigraphic thickness. Assuming that all available accommodation was infilled during the deposition of the Chinle Formation, which is reasonable given the subaerial fluvial and/or shallow-water lacustrine character of these strata, then thickness is a proxy for accommodation, which was controlled locally by tectonic subsidence driven by salt movement at depth.

The Cane Creek anticline is characterized by variable and localized (over 2–3-km; 1.2–1.8-mi) thickness changes between successive lithostratigraphic units (Figure 7), implying that it did not behave as the single anticlinal structure observed today. These thickness changes suggest instead that segments of the underlying salt pillow may have undergone short-lived episodes of evacuation and/or inflation during Chinle Formation deposition, giving rise to spatially and temporally variable accommodation development at the surface.

The lower Chinle and lower-slope units thin gradually onto the flanks of the Moab Valley salt wall (Figures 7A, B; 8), whereas the upper-slope unit thickens into the flanks of the structure (Figures 7C, D; 8). The latter thickness changes suggest salt withdrawal adjacent to the Moab Valley salt wall during upper-slope deposition, consistent with salt flow into the passive-diapiric salt wall. Thickening of the upper-slope unit into the flanks of the Salt Valley salt wall may also be interpreted (Figure 7D).

The Big Bend minibasin is characterized by extreme thickening of the lower Chinle unit toward its center, over an area of approximately 6 × 6 km (3.6 × 3.6 mi) (Figure 7A) (Banbury, 2005). Overlying units exhibit no significant thickening into the minibasin (Figure 7B–D) (Banbury, 2005). Thus, it appears that

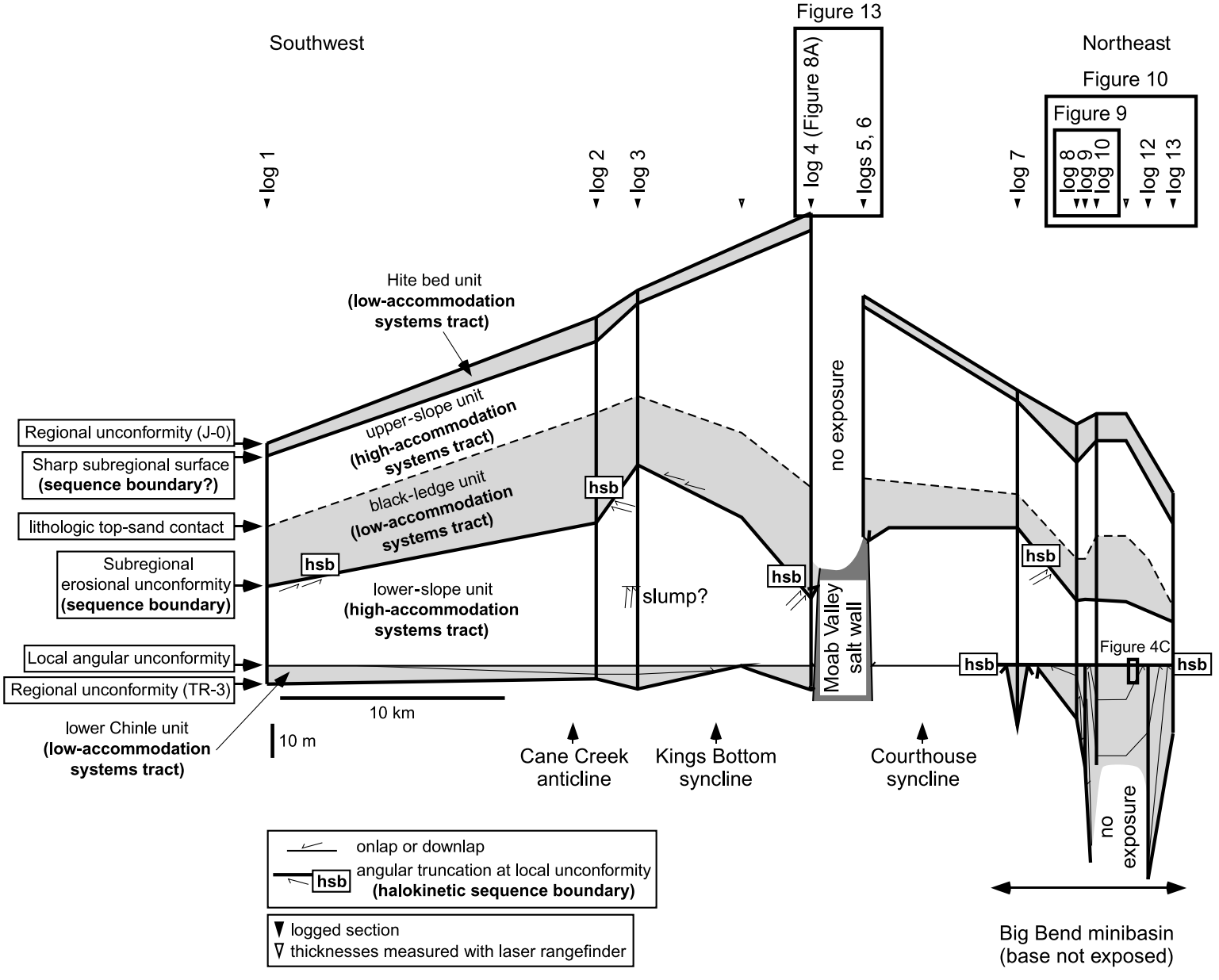

Figure 6. Subregional, southwest-northeast stratigraphic panel for the Chinle Formation, based on field mapping and correlation of measured outcrop sections (modified from Matthews et al., 2004). The panel summarizes major stratigraphic thickness changes and angular stratal relationships across the study area. The panel is located in Figure 1B, and the approximate location of photographs, measured sections, and facies panels in Figures 4C, 8A, 9, 10, and 13 are shown.

the minibasin underwent salt withdrawal during deposition of the lower Chinle unit, but that withdrawal had ceased during deposition of overlying units.

Angular Stratal Relationships

Angular discordances in bedding across regional, subregional, and local unconformities are observed at several locations, described and interpreted below.

The base Chinle unconformity (Figure 5) exhibits an angular discordance with the underlying Moenkopi Formation in the Kane Springs Canyon area (near measured section 14 in Figure 1B) along the northeastern flank of the present-day Cane Creek anticline. Bedding diverges by 12° toward the north-northeast, away from the crest of the anticline. Elsewhere in the study area, the unconformity is not angular.

The upper few meters of the lower Chinle unit are marked by an angular unconformity of up to 20° in the Big Bend minibasin (Figures 5, 9). Beds in the lower Chinle unit dip toward the minibasin center (Figures 6, 7A, 9, 10). The pervasive bioturbation fabric in the lower Chinle unit is perpendicular to bedding, but would originally have been subvertical (Hasiotis, 2002), indicating that bedding was rotated from paleohorizontal prior to truncation at the top lower Chinle unconformity (Figure 4C). Beds in the lower Chinle unit initially increase in dip and thicken toward the center of the minibasin, with the dip angle decreasing to horizontal at the basin center where the lower Chinle unit appears conformable with the overlying lower-slope unit (Figure 10). Angular unconformities are also observed within the lower Chinle unit as its thickness increases into the center of the minibasin, as higher beds with relatively gentle tectonic dips toward the minibasin center truncate lower beds with steeper dips toward the minibasin center (e.g., between logs 8 and 9 in Figure 10). The thinning and pinch-out style of the lower Chinle unit are consistent with the evacuation of salt and the development of a salt-withdrawal minibasin in the Big Bend area (Matthews et al., 2004). Salt evacuation allows strata to thicken into the minibasin and progressively rotate as the base of the minibasin sinks (e.g., Rowan et al., 2003). This interpretation implies that surrounding salt walls (Salt Valley-Cache Valley, Castle Valley, and Moab Valley salt walls; Figures 1B, 7A) acted as prolonged paleotopographic highs at or close to the surface, maintained by passive diapirism during the lower Chinle deposition (Trudgill et al., 2004). The local angular character of the top lower Chinle unconformity reflects the development of paleotopographic relief above the Salt Valley-Cache Valley, Castle Valley, and Moab Valley salt walls during the lower Chinle and/or Moenkopi deposition prior to erosion of the unconformity (Giles and Lawton, 2002; Rowan et al., 2003). Thus, the top lower Chinle unconformity constitutes a halokinetic sequence boundary (sensu Giles and Lawton, 2002) (Figure 6). In other parts of the study area, the only observed angular relationship across the top lower Chinle surface is onlap of beds in the lower-slope unit along the southwestern flank of the Moab Valley salt wall (Figures 7A, 8D, 11). These beds thin and onlap toward the northwest, suggesting that the top lower Chinle surface was slightly tilted toward the southeast (by 0.6°) prior to lower-slope deposition. This tilting likely reflects salt evacuation in the southeast as a result of subsurface salt movement along the strike of the Moab Valley salt wall.

The lower-slope unit on the northeastern flank of the present-day Cane Creek anticline (Figure 7B; Long Canyon and Kane Springs Canyon, corresponding to measured sections 2, 3, and 14 in Figure 1B) contains numerous very localized (<100 m [<330 ft] in lateral extent) unconformities associated with folded, disrupted beds. These unconformities are not correlatable (e.g., Figure 12), and surrounding strata exhibit the prevailing, gentle tectonic dips of the area (<12°). These localized, folded units are interpreted as slumps (Figure 6) (Matthews et al., 2004), implying the presence of nearby paleoslopes. Such paleoslopes may have been generated by subsurface salt movement along the strike of the Cane Creek salt pillow, which would also account for localized thickness changes along the strike of the present-day structure.

The subregional unconformity at the base of the black-ledge unit (Figure 5) is underlain by disrupted beds (facies association 7) across much of the study area (e.g., Figures 4F, G; 6; 8C; 11; 12). Where these beds are folded, they may reflect slumping down paleoslopes, as outlined above in the lower-slope unit. Where the disrupted beds are intensely faulted and fractured, they record brittle deformation of beds that may have undergone early cementation prior to formation of the unconformity, at least locally (Miall and Arush, 2001). On the southwestern flank of the Moab Valley salt wall, the base black-ledge unconformity exhibits a prominent angular discordance between the black-ledge unit above (dipping at 18° toward 190°) and the lower-slope unit below (dipping at up to 42° toward 210°; Figures 7B; 8A–C). Over a distance of several hundred meters, beds in the lower-slope unit thin, become more steeply dipping (dips increase from 25° to >45°), and are truncated

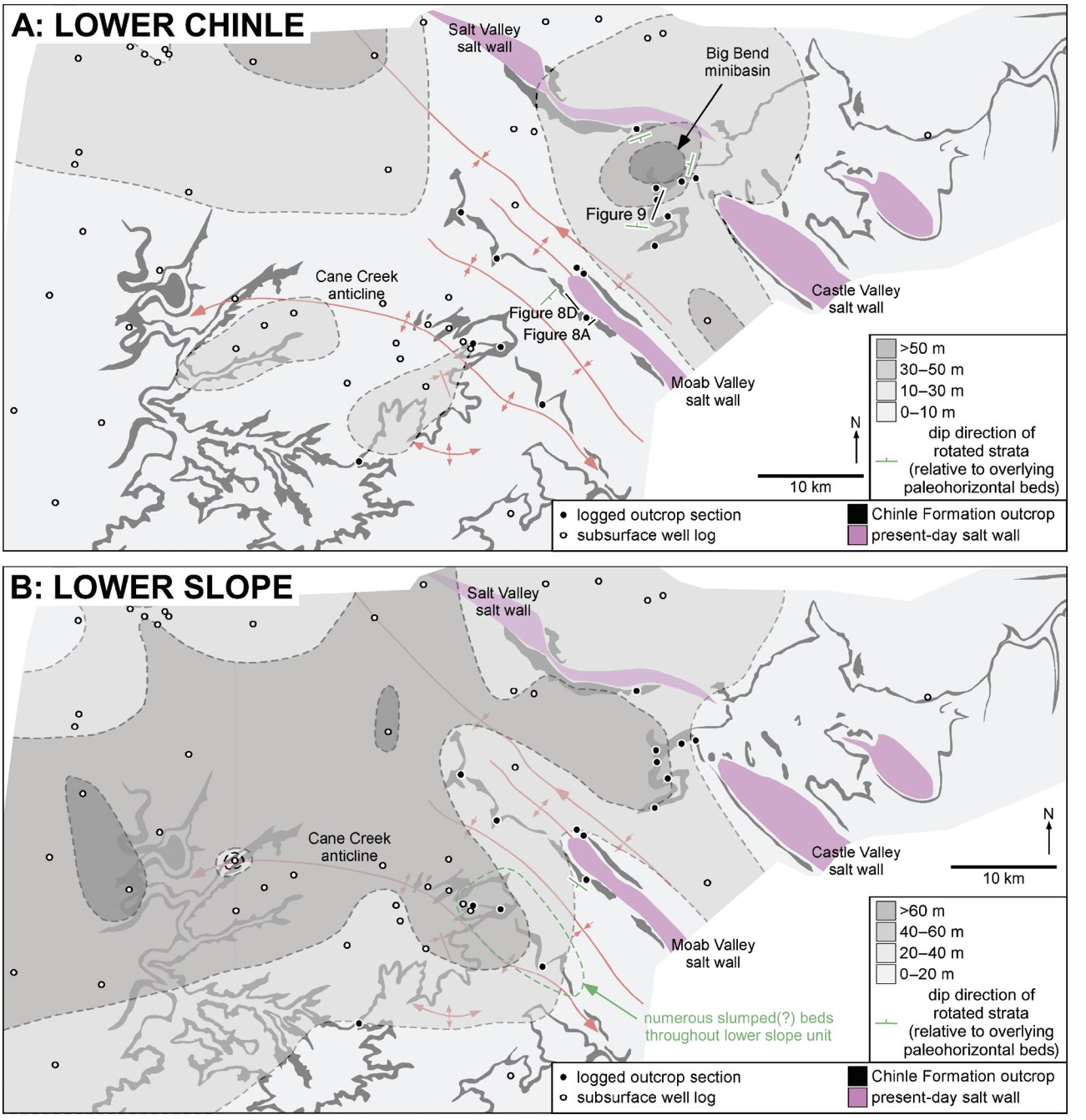

Figure 7. Isopach maps of informal lithostratigraphic units in the Chinle Formation based on outcrop and subsurface data: (A) lower Chinle, (B) lower-slope, (C) black-ledge, and (D) upper-slope units. Maps cover the same area as Figure 1B. Angular discordances in bedding are also shown for each lithostratigraphic unit, relative to restored paleohorizontal defined by beds in the overlying unit.

toward the salt wall (Figure 8A). At meter scale, the beds also thin, curve, and become subparallel to the base black-ledge surface near their truncation toward the salt wall (Figure 8C). The larger scale geometric relationships in the lower-slope unit are consistent with the evacuation of salt, which caused the development of rim synclines around the Moab Valley salt wall (Matthews et al., 2004; Trudgill et al., 2004). Rim syncline development is characterized by thickening and progressive rotation of supersalt strata as salt was evacuated from the base of the syncline (Rowan et al., 2003) in a similar manner to that described for the Big Bend minibasin

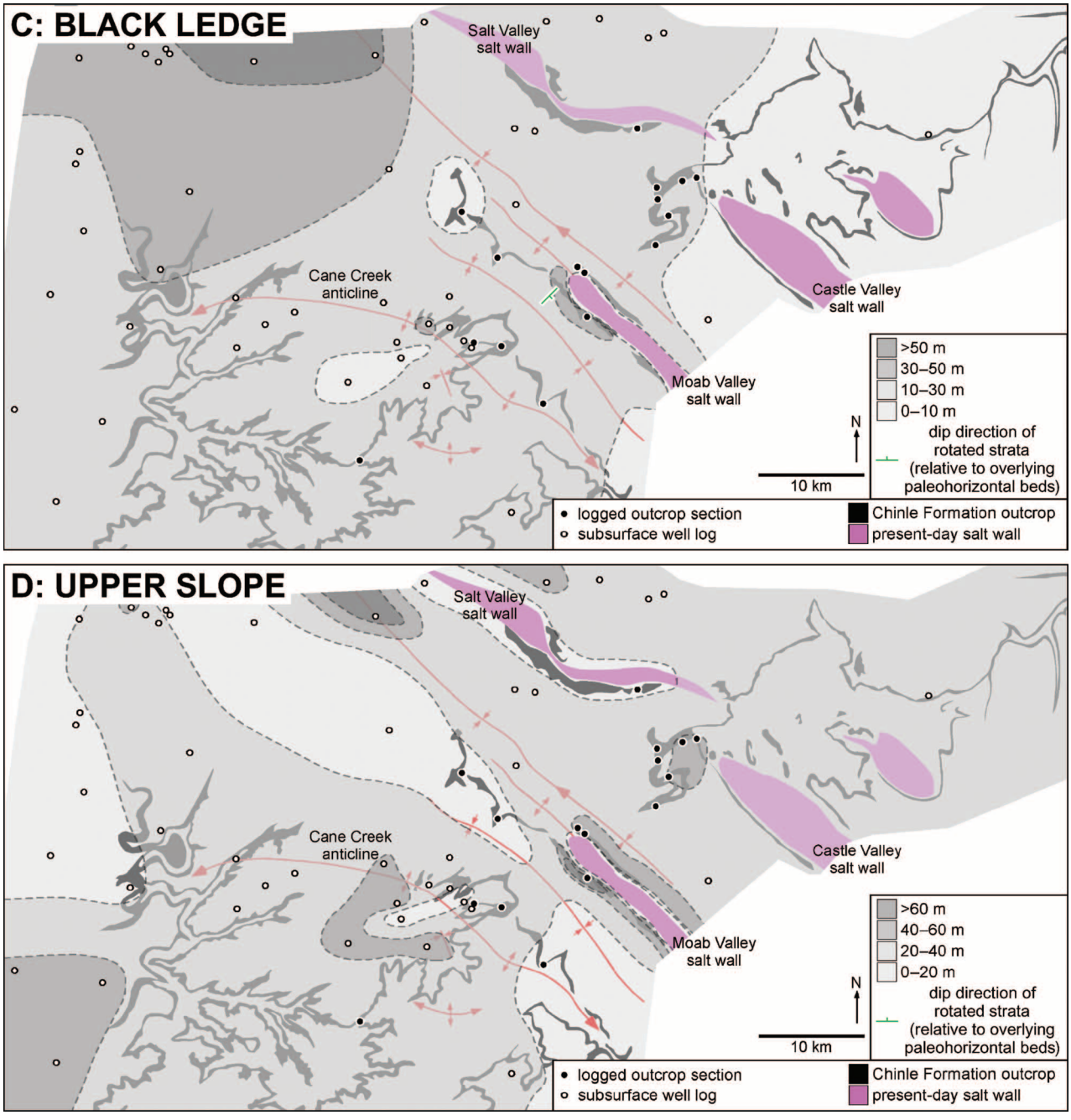

Figure 7. Continued.

above. Thus, the base black-ledge unconformity is also a halokinetic sequence boundary (sensu Giles and Lawton, 2002) (Figure 6). This interpretation requires that the Moab Valley salt wall acted as a prolonged paleotopographic high maintained by passive diapirism during the Late Triassic, as indicated by thinning and pinchout of the Permian–Triassic strata against the Moab Valley salt wall (Doelling, 2001; Trudgill et al., 2004).

The top of the black-ledge unit, although a diachronous surface (Figure 5), is locally marked along the southwestern flank of the Moab Valley salt wall by onlap of overlying beds in the upper-slope unit (Figures 7C, 8D, 11). Onlap suggests that the top of the black-ledge unit was tilted toward the southeast prior to upper-slope deposition, probably reflecting salt evacuation in the southeast. The overlying sequence-stratigraphic surfaces at the base and top of the Hite bed unit (Figure 5) display no strong angular discordances, although the Hite bed unit is interpreted to infill broad, shallow topographic lows (Dubiel, 1987).

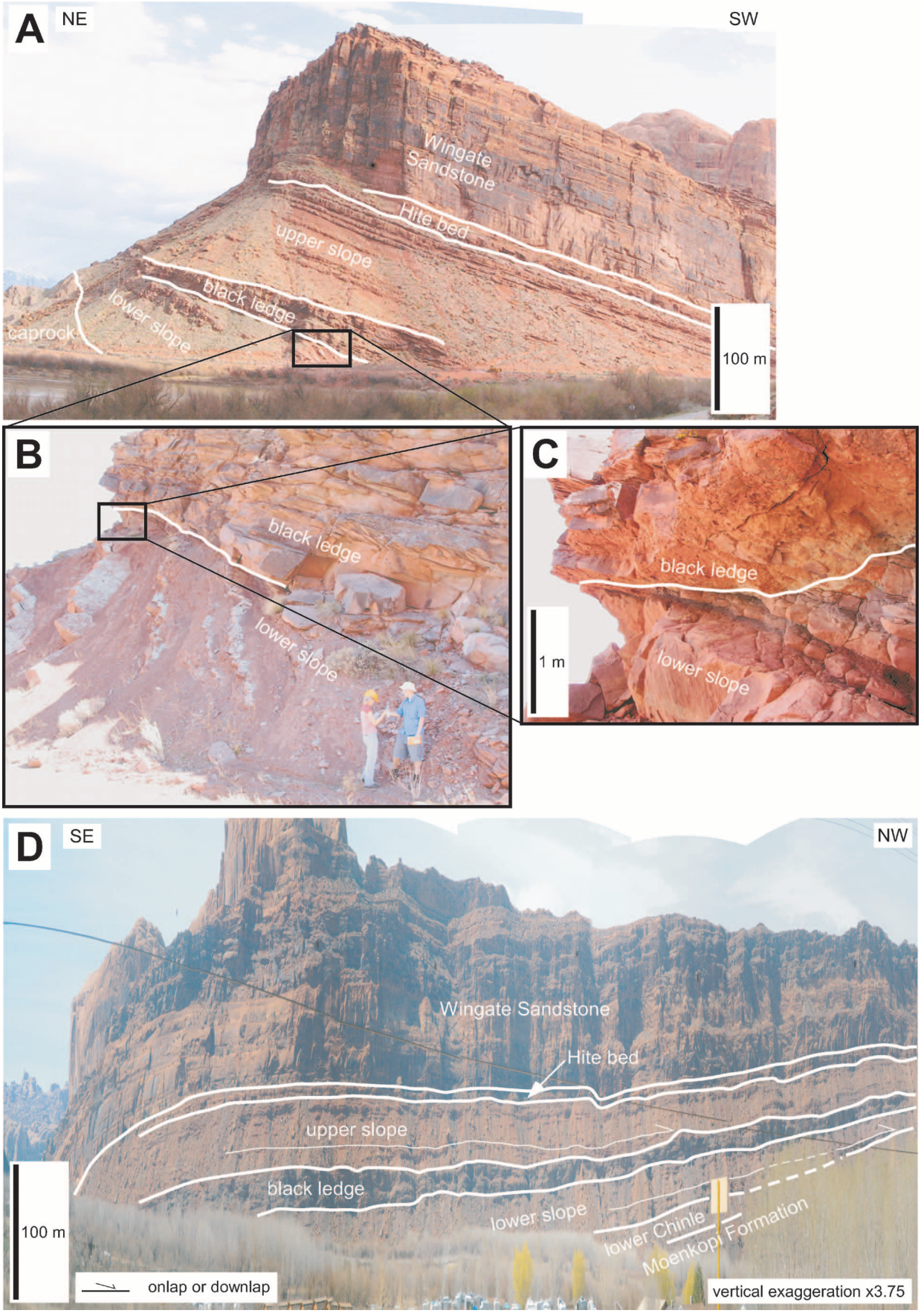
A
NE
SW
Wingate Sandstone
Hite bed
upper slope
black ledge
lower slope
caprock
100 m
B
black ledge
lower slope
C
black ledge
1 m
lower slope
D
SE
NW
Wingate Sandstone
Hite bed
upper slope
black ledge
lower slope
lower Chinle
Moenkopi Formation
100 m
onlap or downlap
vertical exaggeration x3.75

Facies Architecture

Facies architecture around salt structures is best exposed in three areas: (1) along the crest and northeastern flank of the present-day Cane Creek anticline, at Long Canyon (between logs 2 and 3 in Figures 1B, 6) (Hazel, 1994) and Kane Springs Canyon (log 14 in Figures 1B, 12); (2) around the northern part of the Moab Valley salt wall and its anticlinal extension to the northwest (logs 4, 5, 6, 15, and 16 in Figures 1B, 6, 8, 11, 13); and (3) around the southeastern margin of the Big Bend minibasin, along the Colorado River (logs 8, 9, 10, 12, and 13 in Figures 1B, 6, 9, 10). The facies architecture in these three areas is described and interpreted below, from lowest to highest lithostratigraphic units, and placed in the context of interpretive reconstructions of subregional paleogeography (Figure 14).

Within the lower Chinle unit, localized variations in facies architecture are only observed at outcrop in the Big Bend minibasin. The minibasin fill consists predominantly of moderately to completely bioturbated sandstones and mudstones (facies association 4, Figures 10, 14B), which are rare over the rest of the study area. Bioturbation is more intense toward the margins of the minibasin, where beds are thinner. Bioturbation intensity also increases below an angular unconformity 5–15 m (16–49 ft) below the top of the lower Chinle unit (Figure 10). Lacustrine mudstones (facies association 3, Figure 10) also occur above this unconformity near the center of the minibasin. Amalgamated fluvial-channel-fill sandstones and paleosols (facies associations 1 and 5, Figure 10) occur near the minibasin margins, within the lower part of the lower Chinle succession, whereas isolated fluvial-channel-fill sandstones (facies association 1, Figure 10) occur toward the minibasin center within the upper part of the succession. In addition, Prochnow et al. (2005, 2006b) noted truncated, well-drained paleosols at the margin of the minibasin and overthickened, poorly drained paleosols near the minibasin center. Three aspects of this facies architecture are consistent with higher rates of accommodation creation in the minibasin center: (1) reworking of the sediment by bioturbation is more intense near the basin margins, where accommodation creation was slower; (2) paleosol character suggests soil erosion from the well-drained basin margins and sediment transport down a gentle slope toward the low-lying, poorly drained center of the minibasin, where sedimentation rates were faster (Prochnow et al., 2005, 2006b); and (3) lacustrine mudstones occur only in the basin center, where accommodation creation was faster. A minibasinwide stratigraphic control is evident in the abrupt change in bioturbation intensity across the intra–lower Chinle unconformity. Finally, the stacking pattern of fluvial-channel-fill sandstones and development of paleosols may reflect either a stratigraphic control (i.e., denser channel-fill stacking and more mature paleosol development in the lower part of the succession), or a paleogeographic control (i.e., denser channel-fill stacking and more mature paleosol development toward the basin margins, where accommodation creation was slower), or a combination of both controls.

Lower-slope through Hite bed strata in the Big Bend minibasin exhibit only very subtle local variations in facies architecture (e.g., black-ledge paleocurrents are locally directed into the minibasin center; Matthews et al., 2004, p. 945) and instead reflect subregional trends of larger lateral extent than the minibasin (Figure 14C–E). From southwest to northeast, the density of fluvial-channel-fill sandstones (facies association 1) decreases, there is a corresponding increase in the thickness and abundance of lacustrine mudstones in

Figure 8. Photographs illustrating the thickness changes and angular stratal relationships around the Moab Valley salt wall. (A) View of the Chinle Formation on the southwestern flank of the Moab Valley salt anticline at the Colorado River portal (location shown in Figure 7A), showing stratigraphic thinning of the lower-slope and black-ledge units toward the salt wall and stratigraphic thickening of the upper-slope unit toward the salt wall. Note the angular unconformity between the lower-slope and black-ledge units adjacent to the salt wall. The lower-slope unit here rests unconformably on the Paradox Formation cap rock (from Matthews et al., 2004; reproduced with the permission of the Gulf Coast Section SEPM Foundation). (B, C) Detailed views of the lower-slope–black-ledge unconformity. Beds in the lower-slope unit thin, curve, and become subparallel to the overlying unconformity near their truncation toward the salt wall, indicating that the unconformity resulted from syndepositional tectonic rotation. A localized depositional component has also been interpreted for steep dips in the lower-slope unit (lateral accretion deposits within a channel fill; Miall and Arush, 2001, p. 978) (from Matthews et al., 2004; reproduced with the permission of the Gulf Coast Section SEPM Foundation). (D) View from Courthouse Wash of the southwestern flank of the Moab Valley salt anticline (location shown in Figure 7A), with vertical exaggeration of $\times 3.75$. The lower Chinle, lower-slope, and upper-slope units all thin stratigraphically toward the northwest, in part because of onlap onto the basal surfaces of the lower-slope and upper-slope units. Note that the photomontage contains perspective effects because its northwestern end is farther from the viewer.

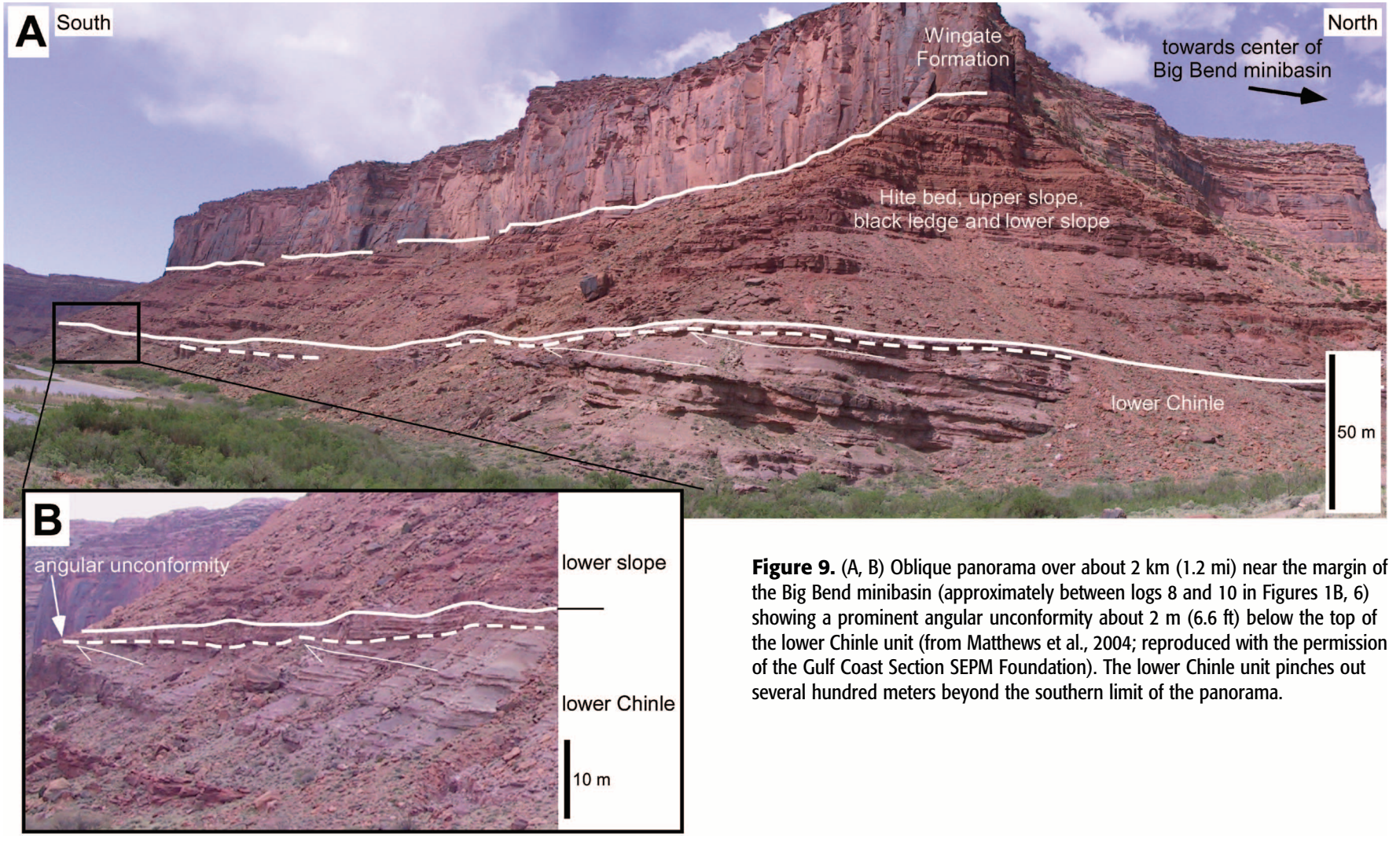

Figure 9. (A, B) Oblique panorama over about 2 km (1.2 mi) near the margin of the Big Bend minibasin (approximately between logs 8 and 10 in Figures 1B, 6) showing a prominent angular unconformity about 2 m (6.6 ft) below the top of the lower Chinle unit (from Matthews et al., 2004; reproduced with the permission of the Gulf Coast Section SEPM Foundation). The lower Chinle unit pinches out several hundred meters beyond the southern limit of the panorama.

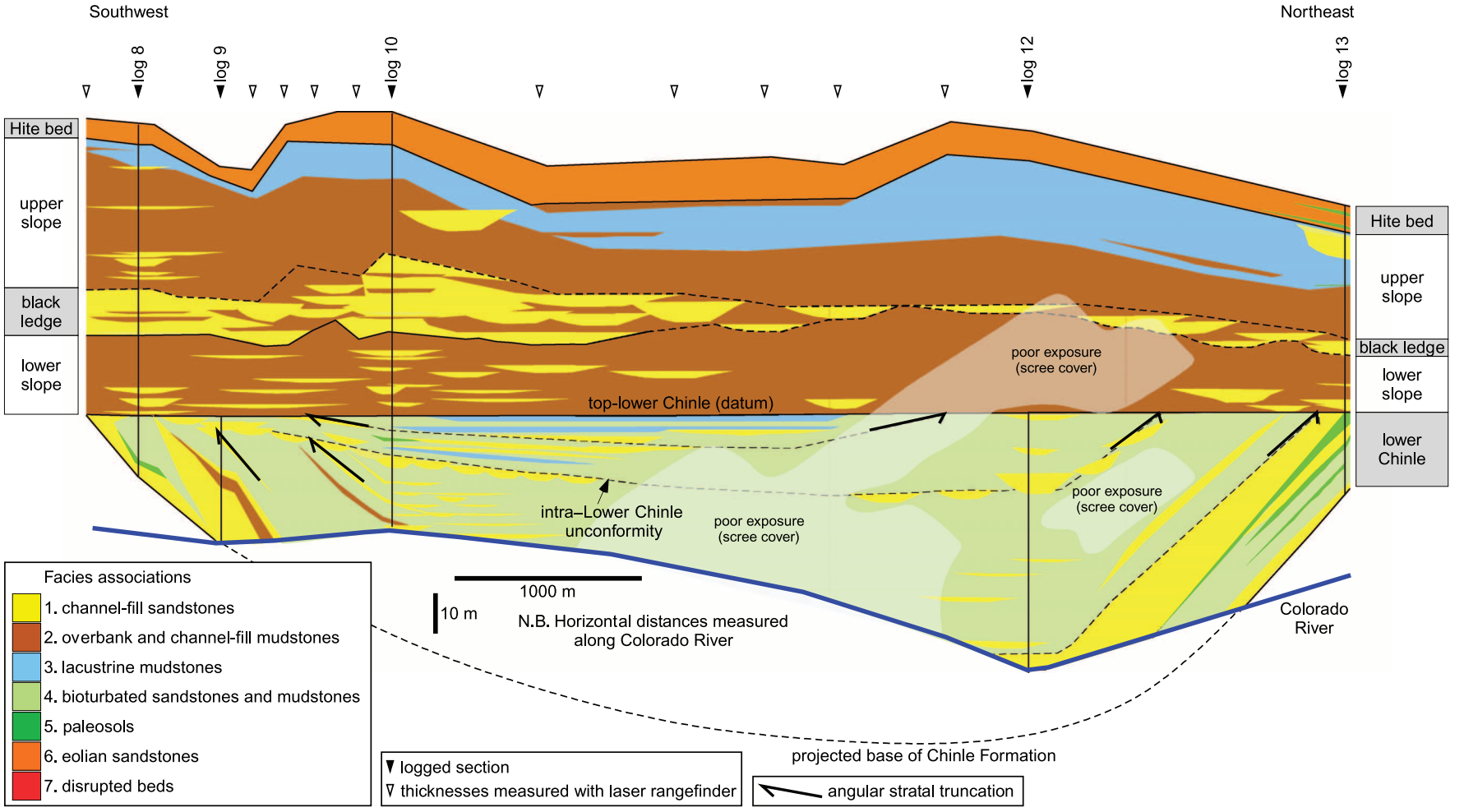

Figure 10. Facies architecture panel along the northern side of the Colorado River across the Big Bend minibasin (between logs 8, 9, 10, 12, and 13 in Figures 1B, 6). The panel lies along the southeastern margin of the minibasin.

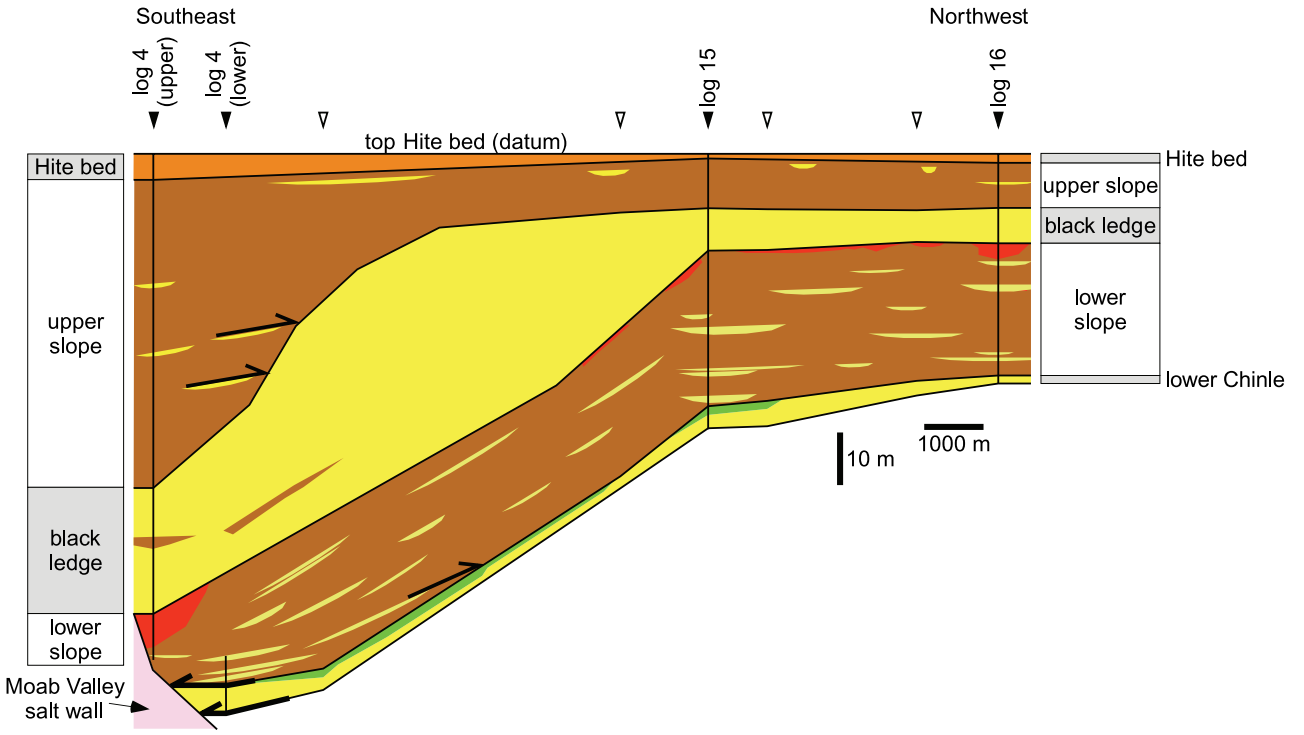

Figure 11. Facies architecture panel along the southwestern flank of the Moab Valley salt wall and its subsurface extension to the northwest as a salt-cored anticline (between measured sections 4, 15, and 16 in Figure 1B). The panel follows the cliff face exposed in the footwall of the Moab fault. Key is as in Figure 10.

the upper-slope unit (facies association 2), and the black-ledge unit thins and becomes less distinct (Figure 10). These trends suggest decreasing proximity to fluvial-channel belts toward the northeast. The dominance of subregional controls on facies architecture is consistent with the relatively uniform thickness of these strata, the absence of angular stratal relationships, and the uniform character of paleosols across the minibasin (Prochnow et al., 2005, 2006b), all of which suggest that growth of the Big Bend minibasin slowed significantly or terminated after lower Chinle deposition.

The lower-slope unit contains a high proportion of folded, disrupted beds (facies association 7), interpreted as slump deposits, along the crest and northeastern flank of the present-day Cane Creek anticline (Figures 10, 14C). Both isolated and multistory fluvial-channel-fill sandstones (facies association 1) in the unit also contain a high proportion of gravel-grade, intra- and extraformational clasts here. Multistory fluvial-channel-fill sandstones (e.g., ''Kane Springs 1'' and ''Kane Springs 3'' sand bodies of Hazel, 1991, 1994) trend parallel to the crest of the anticline (Figure 14C). Paleocurrents on the southwestern flank of the Moab Valley salt wall are directed toward the southwest (Figure 13), indicating local fluvial drainage away from the salt wall and toward the northeastern flank of the present-day Cane Creek anticline (Figure 14C). These observations suggest the development of an axial fluvial drainage toward the northwest, in response to the uplift of the Cane Creek salt pillow and Moab Valley salt wall, with localized sediment influx from the paleoslopes on the flanks of these structures (Hazel, 1994). The abundance of slump deposits supports the development of paleoslopes above the Cane Creek salt pillow, whereas intra- and extraformational gravels have most likely been eroded from paleotopographic highs above the Cane Creek salt pillow and Moab Valley salt wall (Hazel, 1994). The Moab Valley salt wall may have been the nearest source of the extraformational gravels because Pennsylvanian through Lower Triassic strata (Paradox, Honaker Trail, Cutler, and Moenkopi formations) were probably exposed discontinuously along its southwestern flank. In other parts of the study area, the lower-slope unit conforms to subregional facies trends of larger lateral extent than individual salt structures (Figures 14C).

At a subregional scale, the multistory fluvial-channel-fill sandstones of the black-ledge unit thin and pass laterally into overbank mudstones east of the Big Bend minibasin and Castle Valley salt wall (Figures 10, 14D). More locally, the unit exhibits a relatively uniform

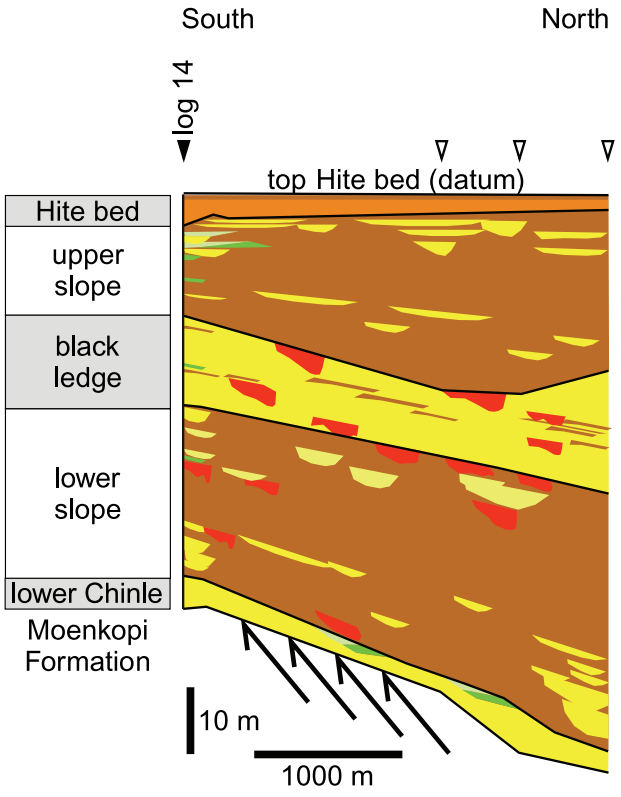

Figure 12. Facies architecture panel along the northwestern side of Kane Springs Canyon from the crest of the present-day Cane Creek anticline (south; measured section 14 in Figure 1B) down its northeastern flank (north). Key is as in Figure 10.

facies architecture and high sandstone content (>90%) across all the salt structures despite changes in its thickness (Figures 11–13). Slightly increased proportions of overbank and channel-fill mudstones are noted locally in areas of greater thickness, reflecting the higher preservation potential of these deposits in areas of faster accommodation creation (Matthews et al., 2004), but this effect is subtle. Paleocurrents within the unit are widely variable (Figure 14D), consistent with its deposition by braided fluvial systems (Miall, 1978). In general, local paleocurrent distributions indicate that fluvial systems were not deflected around growing paleotopographic highs above salt pillows and walls, but instead flowed directly across them (e.g., paleocurrents on both flanks of the Moab Valley salt wall are directed toward the southwest; Figures 13, 14D). These observations suggest that the black-ledge braided fluvial system continuously eroded and/or dissolved paleotopographic highs generated above salt pillows and walls during its deposition (Matthews et al., 2004). Such erosion is supported by the occurrence of reworked clasts of older Chinle Formation strata within the black-ledge unit (e.g., around the Moab Valley salt wall; Doelling et al., 2002). A localized exception occurs on the southern flank of the Cache Valley salt wall and the northwestern tip of the Castle Valley salt wall, where paleocurrents are directed into the center of the Big Bend minibasin (Figure 14D), implying that the minibasin still formed a subtle paleotopographic low during black-ledge deposition (Matthews et al., 2004). Such a paleotopographic low may have resulted from a final, minor episode of salt evacuation below the basin and/or from compaction of the older basin-fill strata.

The upper-slope unit generally follows subregional facies trends that extend across individual salt structures (Figure 14E). The strongest locally variable facies architecture occurs around the Moab Valley salt wall. On the northeastern flank of the salt wall, the upper-slope unit is dominated by stacked, fluvial-channel-fill sandstones, with paleocurrents oriented toward the north, whereas on its southern flank, the unit contains a much higher proportion of overbank mudstones, and paleocurrents in isolated fluvial-channel-fill sandstones are oriented toward the southwest (Figure 13). These differences suggest that the salt wall acted as a paleotopographic high, separating two discrete, rim-syncline depocenters that contain thickened upper-slope strata (Figures 6, 7D). The occurrence of reworked clasts of older Chinle Formation strata in the upper-slope unit adjacent to the Moab Valley salt wall (Doelling et al., 2002) implies continued uplift and erosion on the flanks of the salt wall during its deposition. Paleocurrents on the crest and northeastern flank of the present-day Cane Creek anticline are directed to the north and northeast (Figure 14E), implying that there may have also been a paleotopographic high above the Cane Creek salt pillow (as during deposition of the lower-slope unit; Hazel, 1994). This interpretation is supported by the occurrence of paleosols in thin upper-slope sections on the crest of the structure and their absence in thickened sections down the flanks (Figure 12).

Timing and Style of Salt Movement during Chinle Formation Deposition

The three indicators described above constrained the timing and style of salt movement during deposition of the Chinle Formation. Salt-tectonic style was well established prior to Chinle Formation deposition and consisted predominantly of steep-sided salt walls (Moab Valley, Salt Valley-Cache Valley, Castle Valley, and Onion Creek salt walls, Figure 1B). Salt walls were

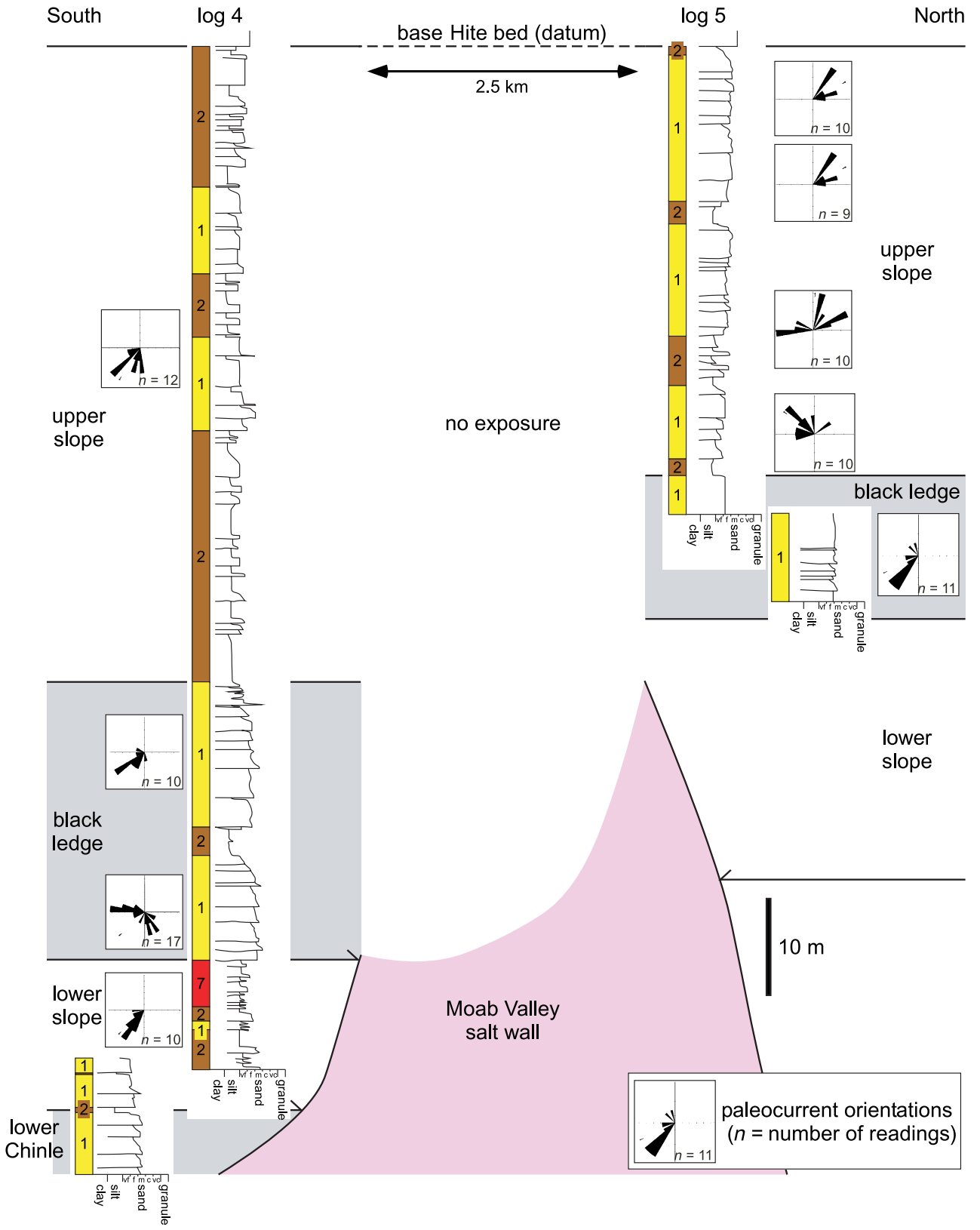

Figure 13. Measured sections through the black-ledge and upper-slope units from the southwestern and northeastern flanks of the Moab Valley salt anticline (logs 4 and 5 in Figures 1B, 6, respectively), illustrating differences in thickness, facies architecture, and paleoflow across the structure (modified from Matthews et al., 2004; reproduced with the permission of the Gulf Coast Section SEPM Foundation). Key is as in Figure 10.

maintained at, or close to, the surface by passive diapirism, which required a subsurface flow of salt from adjacent rim synclines and minibasins (Trudgill et al., 2004). The Chinle Formation records the decline of such salt movement over most of the study area (Trudgill et al., 2004; Banbury, 2005). Significant growth of the Big Bend minibasin ceased after the deposition of the lower Chinle unit (e.g., Figure 7), implying the end of salt evacuation and flow into the adjacent Cache Valley, Castle Valley, and Moab Valley salt walls. Stratal thickening into rim synclines adjacent to the Moab Valley salt wall ceased after the deposition of the upper-slope unit (e.g., Figures 6, 8A), implying the end of passive diapirism there. In contrast, subsurface well data suggest that rim synclines containing thickened strata were initiated adjacent to the northern part of the Salt Valley salt wall during upper-slope deposition, implying the onset of passive growth of this structure (Figures 7D, 14E). The end of passive diapirism most likely reflects the development of localized salt welds, with overlying strata grounding out on subsalt basement, which terminated salt flow into the salt walls. For example, the end of salt evacuation below the Big Bend minibasin likely represents the development of an underlying salt weld that isolated the Moab Valley and Salt Valley salt walls from each other (Trudgill et al., 2004; Banbury, 2005).

A key feature of salt tectonism during Chinle Formation deposition is along-axis salt flow in individual structures, expressed as subtle thickening and tilting of strata above localized segments of salt pillows and buried salt walls (e.g., above the Cane Creek salt pillow, Figure 7, and the salt pillow extending northwest of the Moab Valley salt wall, Figures 7, 8D, 11). These stratal geometries were formed in response to fluctuating topographic relief above the salt pillows and buried salt walls. Along-axis salt flow of this type implies a small salt volume within the structures, compatible with the development of localized salt welds that restricted salt input from adjacent areas. For example, salt flow along the Cane Creek salt pillow and Moab Valley salt wall may have been enhanced by the isolation of these two structures (which are not separated by a salt weld and, thus, shared a common salt supply; Trudgill et al., 2004) from the Salt Valley salt wall by the grounding out of the intervening Big Bend minibasin. In this interpretation, the Moab Valley salt wall was maintained at the surface during the deposition of lower-slope to upper-slope strata, while northwesterly segments of the Cane Creek salt pillow ceased to inflate, consistent with a common but restricted salt supply for the two structures.

PREDICTION OF RESERVOIR DISTRIBUTION AND ARCHITECTURE: DISCUSSION

Our observations and interpretations of the Chinle Formation are synthesized in two predictive models of fluviolacustrine facies architecture in evolving salt basins (Figure 15). The models emphasize the interaction of controls at regional (e.g., regional tectonic subsidence and stratigraphic architecture; Blakey and Gubitosa, 1984) and local scales (e.g., paleotopography and accommodation induced by salt movement; Prochnow et al., 2005, 2006b), within the context of a series of passive salt walls undergoing relatively subdued growth.

The first model is for either a low-energy fluvial system or a fluvial system developed under a relatively high regional accommodation regime (e.g., lower-slope and upper-slope units; high-accommodation systems tract; Figure 15A). The key aspect of this model is that salt walls and inflating salt-pillow segments were expressed at the surface as topographic highs that imparted a strong local control on sediment dispersal and resulting facies distributions. Isolated fluvial-channel-fill sandstones were locally stacked into belts that record axial drainage between the topographic highs. The net-to-gross sand ratio is relatively high in the resulting sand fairways (up to 60%), but is low (20–30%) outside of them. Salt-withdrawal depocenters developed in rim synclines, and minibasins either host channel-belt sand fairways or lacustrine mudstones, depending on the subregional configuration of fluvial drainage. This model is similar to that developed by Smith et al. (1993) for Middle Triassic (TR20) fluviolacustrine strata in the salt province of the central North Sea Basin (United Kingdom), although our model incorporates additional aspects of local paleosol development, slumping down paleoslopes, and angular stratal relationships that enable a more refined interpretation of subsurface data. Equivalent shallow-marine strata are characterized by sand shoals above topographic highs and tidal embayments within salt-withdrawal minibasins (Aschoff and Giles, 2005; Shelley and Lawton, 2005), demonstrating the strong influence of salt-driven submarine bathymetry.

The second model is for either a high-energy fluvial system or a fluvial system developed under a relatively low regional accommodation regime (e.g., black-ledge unit, low-accommodation systems tract; Figure 15B), in which the fluvial system was able to erode and/or dissolve growing topographic highs above salt walls and inflating salt-pillow segments. As a result, there was little local control on sediment dispersal and resulting facies distributions, although preserved thickness was controlled

Figure 14. (A) Regional paleogeography of the Upper Triassic Chinle Formation (from Hazel, 1994; Blakey, 1997). Interpretive reconstructions of subregional paleogeography in the northeastern Paradox Basin are shown for the following units (Figure 5): (B) lower Chinle, (C) lower slope, (D) black ledge, and (E) upper slope.

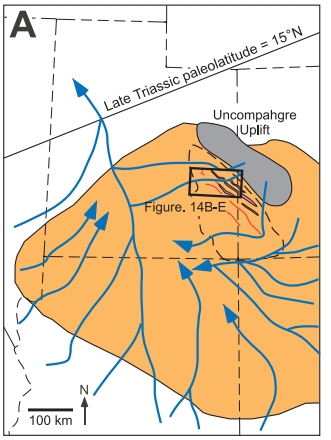

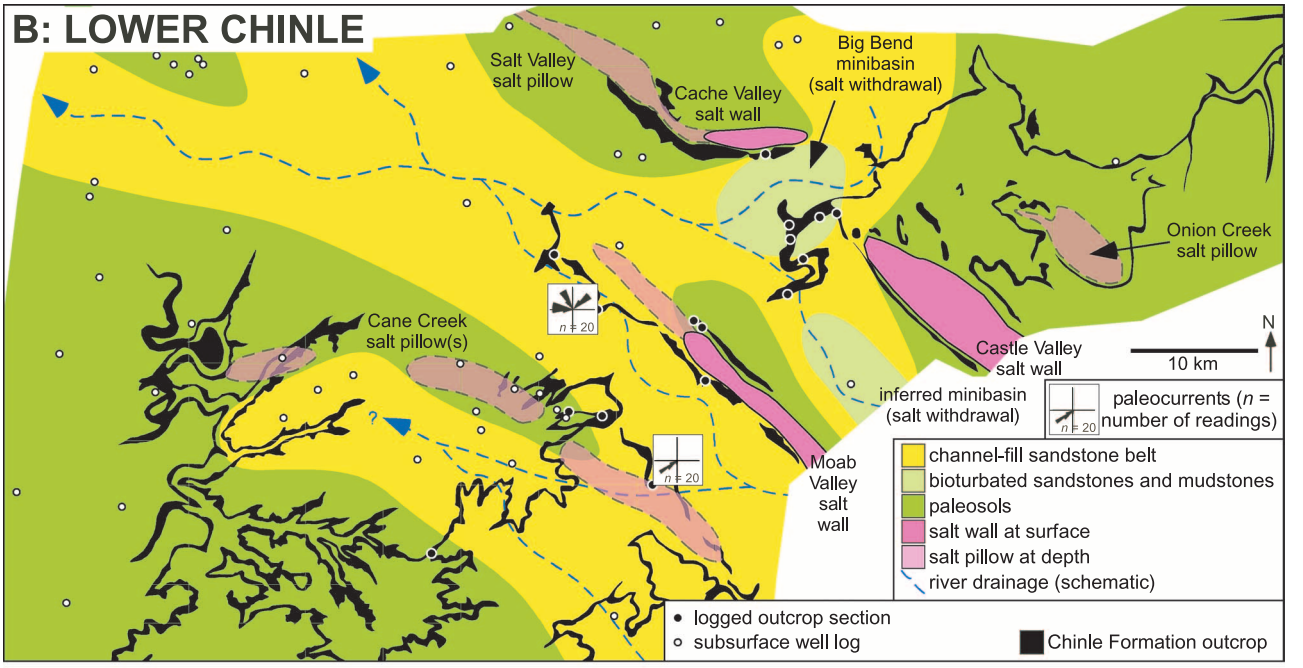

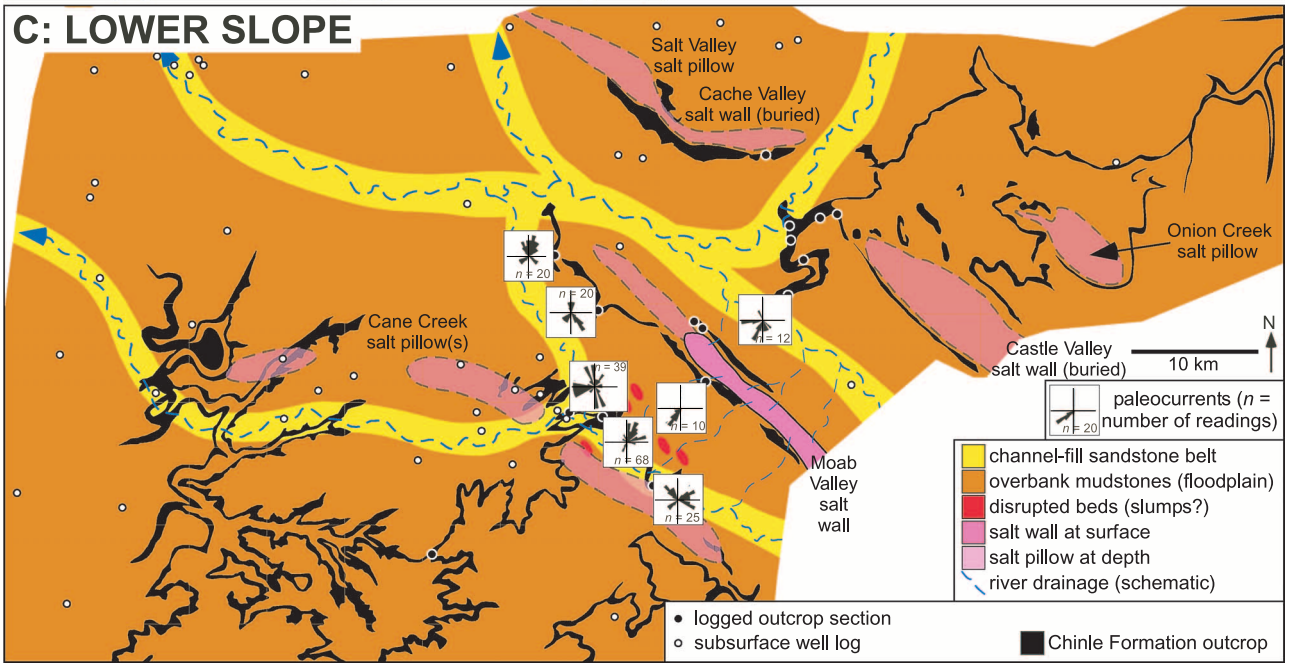

by the differential creation of accommodation across the growing salt structures. Braided fluvial systems were widespread across the area, resulting in deposition of a high net-to-gross (80–100%) sandstone sheet. Salt-withdrawal depocenters that developed in rim synclines and minibasins were areas of rapid accommodation creation, and they contain expanded strata and laterally discontinuous mudstones that are the preserved remnants of overbank deposits. Salt walls were areas of zero accommodation, and they were characterized by sediment bypass and nondeposition. This model has some similarities to those developed for similar fluviolacustrine deposits in passive salt diapir settings by Smith et al. (1993) for Late Triassic (TR30) strata in the central North Sea Basin (United Kingdom) and by Barde et al. (2002a, b) for Permian–Triassic strata in the Precaspian Basin (Kazakhstan and Russia). One critical difference is that our model predicts the presence of sand sheets directly adjacent to passively growing salt walls. Continued growth of the salt walls would result in the

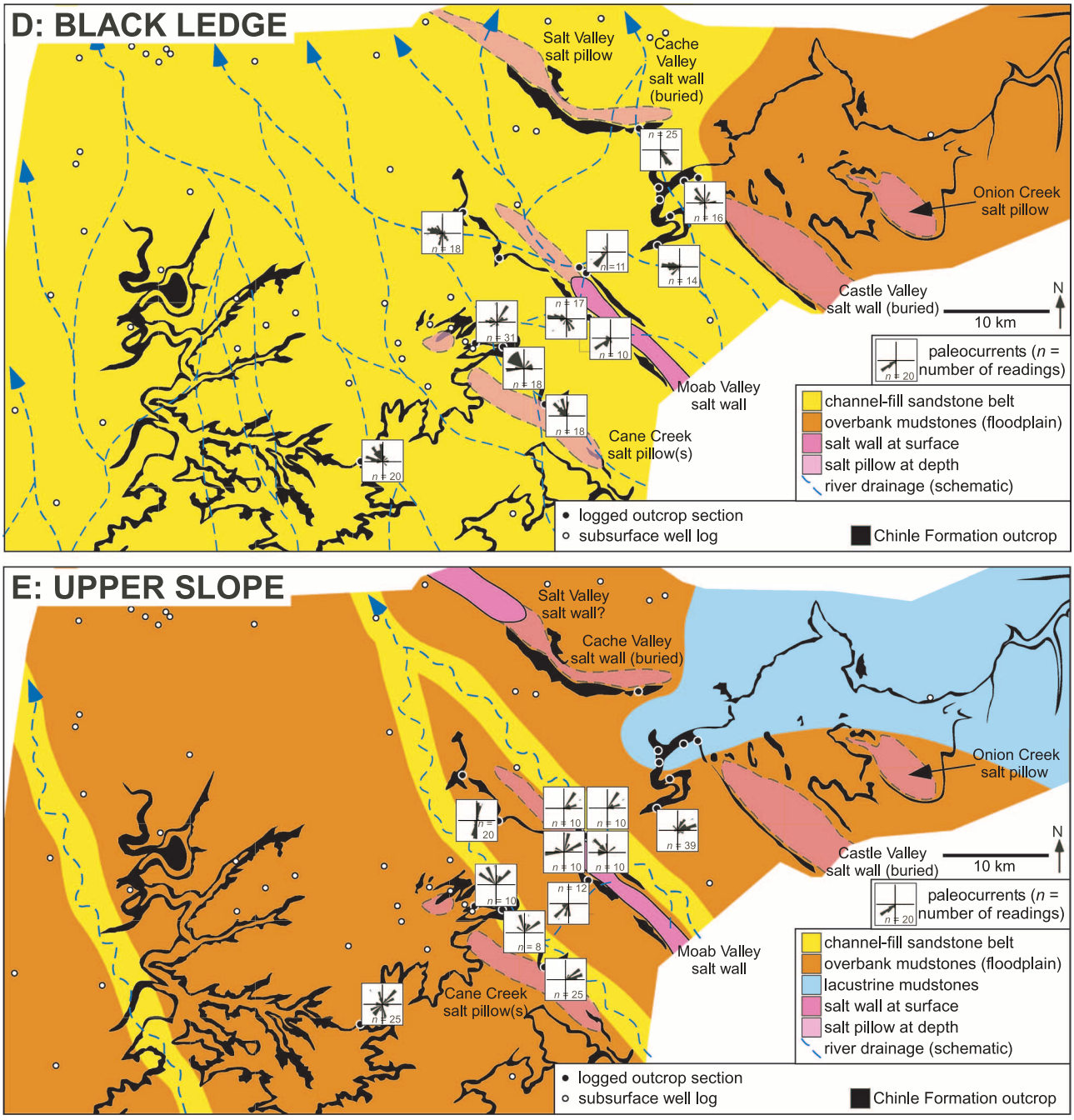

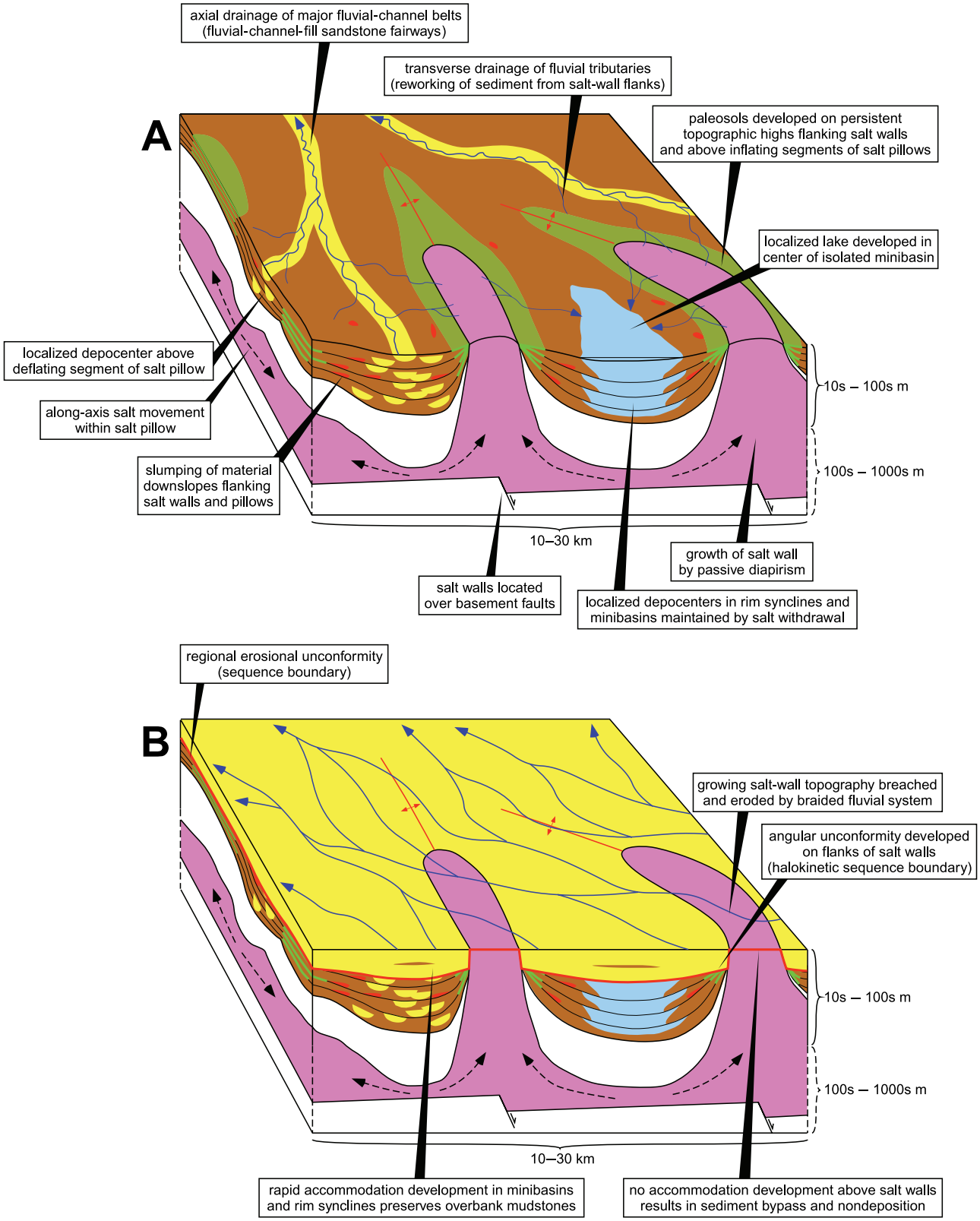

Figure 15. Conceptual models of facies distributions, stratal geometries, and thickness variations in fluviolacustrine strata based on the Chinle Formation, northeastern Paradox Basin: (A) high-accommodation systems tract (e.g., lower-slope and upper-slope units), (B) low-accommodation systems tract (e.g., black-ledge unit). Facies key is as in Figure 10.

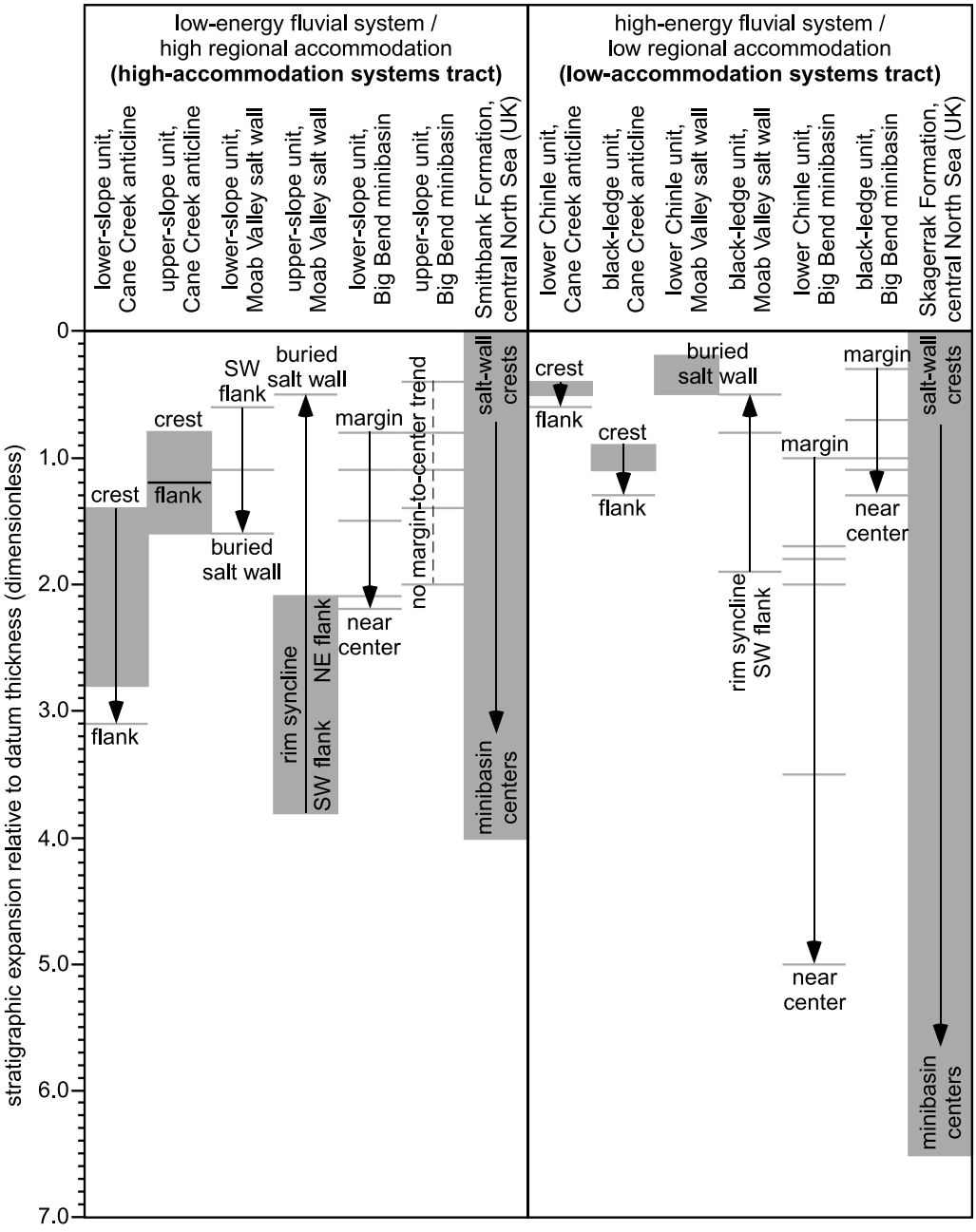

Figure 16. Stratigraphic expansion across salt structures in the Chinle Formation, northeastern Paradox Basin, and in the Smith Bank and Skagerrak formations, central North Sea (United Kingdom; compiled from data in Goldsmith et al., 2003). These data suggest that both intervals of fluviolacustrine strata underwent a comparable degree of stratigraphic expansion in response to passive salt diapirism.

rotation of the sand sheet such that it dips down the salt-wall flanks (e.g., Figure 8A). Thus, the model predicts that salt-wall flanks contain high-quality reservoir sands in a viable structural-trapping configuration, assuming an updip seal against the salt wall.

Can the models described above for relatively thin intervals (several tens of meters in the Chinle Formation) be applied to thicker packages of strata (e.g., hosting Triassic plays in the central North Sea Basin, United Kingdom, and Permian–Triassic plays in the Precaspian Basin, Kazakhstan, and Russia; Smith et al., 1993; Stewart and Clark, 1999; Barde et al., 2002a, b; Goldsmith et al., 2003; Volozh et al., 2003)? This question is addressed by considering the degree of stratigraphic expansion across the salt structures relative to a datum thickness unaffected by salt tectonics (e.g., log 1 in Figure 1B for the Chinle Formation). This measure of stratigraphic thickness variability suggests that our model for low-energy fluvial systems and/or high regional accommodation regime (Figure 15A) applies for stratigraphic expansion up to four times (Figure 16). Our model for high-energy fluvial systems and/or low regional accommodation regime (Figure 15B) is based explicitly on the black-ledge unit, but it also applies to the

lower Chinle unit everywhere except the Big Bend minibasin. This suggests that the model applies for stratigraphic expansion up to two times (Figure 16), but may break down at larger stratigraphic expansions. For example, the lower Chinle unit in the Big Bend minibasin exhibits up to five times the stratigraphic expansion at outcrop, but there, channel-fill sandstones are interspersed with overbank mudstones, and both are heavily overprinted by bioturbation (Figures 4C, 9). For comparison, stratigraphic expansion of the Triassic mudstone-dominated Smith Bank and sandstone-bearing Skagerrak formations in the central North Sea ranges up to 4 and 6.5 times, respectively (Figure 16) (compiled from data in Goldsmith et al., 2003). This comparison suggests that the models presented here (Figure 15) are directly applicable to the Smith Bank Formation and gently thickened Skagerrak Formation sections (stratigraphic expansion less than two times), but should be applied with care to strongly thickened sections of the Skagerrak Formation (e.g., rim-syncline and minibasin depocenters with stratigraphic expansion greater than two times). The applicability of the models (Figure 15) is supported by the occurrence of widespread sandstone-dominated and mudstone-dominated lithostratigraphic members in the Skagerrak Formation (Goldsmith et al., 2003), which suggests that regional controls exert a strong influence on stratigraphy, similar to the Chinle Formation.

CONCLUSIONS

The evidence of deposition during growth of passive salt diapirs is provided by (1) stratigraphic thickness variations, (2) angular stratal relationships, and (3) localized facies architecture. These criteria reveal subtle variations in the evolution of diapirs and related structures that influenced sediment dispersal patterns. For example, the timing of salt-weld development controlled the subregional growth patterns of rim-syncline and minibasin depocenters, whereas along-axis salt flow in salt walls and buried salt pillows created short-lived, localized depocenters on the crests of these structures. Such subtle variations have limited predictability from present-day salt-body geometries and, in the subsurface, may be best addressed via structural restoration of synkinematic growth strata.

Reservoir distribution and architecture reflects a complex interplay between regional, subregional, and local controls on sedimentation, but two predictive models are synthesized. (1) Low-energy fluvial systems and/or relatively high regional accommodation regimes (high-accommodation systems tracts) were controlled by localized, salt-induced topography. Fluvial sand fairways are confined to the axes of rim synclines, minibasins, and deflating salt-pillow segments (i.e., areas of salt withdrawal) that were occupied by regional fluvial-drainage systems. (2) High-energy fluvial systems and/or relatively low regional accommodation regimes (low-accommodation systems tracts) exhibit less local variability because rivers could breach and erode salt-induced topography. Such strata are characterized by widespread sheet sandstones that thicken in areas of salt withdrawal. These models have applications in fluviolacustrine, salt-province plays with at least four times stratigraphic expansion (low-energy fluvial system and/or high regional accommodation regime) and up to two times stratigraphic expansion (high-energy fluvial system and/or low regional accommodation regime).

Three key aspects of the outcrop-derived models for reservoir prediction are as follows.

1. Subregional to regional sequence-stratigraphic frameworks can be extended into areas of moderate stratigraphic expansion (up to four times) because of passive salt diapirism. The application of such frameworks allows the identification of high-accommodation and low-accommodation systems tracts, which have different styles of reservoir distribution in areas of salt withdrawal.
2. Sand fairways in high-accommodation systems tracts are confined to areas of expanded stratigraphic section containing regional fluvial-drainage systems. Reconstruction of regional paleodrainage patterns is essential to identify these sand fairways. Many areas of expanded stratigraphic section occur within synclines that developed by continued passive salt withdrawal, and thus, stratigraphic trapping is likely to be an important component of successful plays in these systems tracts.
3. Reservoir distribution is more widespread in low-accommodation systems tracts, and fluvial sheet sandstones developed in these systems tracts are likely to abut, or pinch out close to, passive salt walls. Where these structures continued to passively grow after deposition of the low-accommodation systems tracts, sheet sandstones are likely to dip down the salt-wall flanks, thus producing a viable structural-trapping configuration with an updip seal against the salt wall.

This study demonstrates the value of outcrop analogs in developing concepts and models for constraining subseismic reservoir distribution and architecture in complex depositional settings, such as salt basins. Models developed from such analogs may be readily tested against seismic and well data.

REFERENCES CITED

Ahlbrandt, T. S., and S. G. Fryberger, 1981, Sedimentary features and significance of interdune deposits, *in* F. G. Etheridge and R. M. Flores, eds., Recent and ancient nonmarine depositional environments: Models for exploration: SEPM Special Publication 31, p. 293–314.

Aschoff, J. L., and K. A. Giles, 2005, Salt diapir-influenced, shallow-marine sediment dispersal patterns: Insights from outcrop analogs: AAPG Bulletin, v. 89, p. 447–469.

Banbury, N. J., 2005, The role of salt mobility in the development of supra-salt sedimentary depocentres and structural styles: Ph.D. thesis, University of Edinburgh, Edinburgh, United Kingdom, 298 p.

Barbeau, D. L., 2003, A flexural model for the Paradox Basin: Implications for the tectonics of the Ancestral Rocky Mountains: Basin Research, v. 15, p. 97–115.

Barde, J.-P., P. Chamberlain, M. Galavazi, P. Gralla, J. Harwijanto, J. Marsky, and F. Van Den Belt, 2002a, Sedimentation during halokinesis: Permo-Triassic reservoirs of the Saigak field, Precaspian Basin, Kazakhstan: Petroleum Geoscience, v. 8, p. 177–187.

Barde, J.-P., P. Gralla, J. Harwijanto, and J. Marsky, 2002b, Exploration of the eastern edge of the Precaspian Basin: Impact of data integration on Upper Permian and Triassic prospectivity: AAPG Bulletin, v. 86, p. 399–416.

Barton, D. C., 1933, Mechanics of formation of salt domes with special reference to Gulf Coast salt domes of Texas and Louisiana: AAPG Bulletin, v. 17, p. 1025–1083.

Blakey, R. C., 1997, Paleogeography of the southwestern US: http://jan.ucc.nau.edu/~rcb7/paleogeogwus.html (accessed March 31, 2003).

Blakey, R. C., and R. Gubitosa, 1984, Controls of sandstone body geometry and architecture in the Chinle Formation (Upper Triassic), Colorado Plateau: Sedimentary Geology, v. 38, p. 51–86.

Bromley, M. H., 1991, Architectural features of the Kayenta Formation (Lower Jurassic), Colorado Plateau, U.S.A.: Relationship to salt tectonics in the Paradox Basin: Sedimentary Geology, v. 73, p. 77–84.

Cant, D. J., and R. G. Walker, 1978, Fluvial processes and facies sequences in the sandy braided south Saskatchewan River, Canada: Sedimentology, v. 25, p. 625–648.

Doelling, H. H., 1988, Geology of Salt Valley anticline and Arches National Park, Grand County, Utah, *in* H. H. Doelling, C. G. Oviatt, and P. W. Huntoon, eds., Salt deformation in the Paradox region: Utah Geological and Mineral Survey Bulletin, v. 122, p. 1–58.

Doelling, H. H., 2000, Geologic road and trail guides to Arches National Park, Utah, *in* P. B. Anderson and D. A. Sprinkel, eds., Geologic road, trail, and lake guides to Utah's parks and monuments: Utah Geological Association Publication 29, CD-ROM.

Doelling, H. H., 2001, Geologic map of the Moab and eastern part of the San Rafael Desert 30′ by 60′ quadrangles, Grand and Emery counties, Utah and Mesa County, Colorado: Utah Geological Survey Map 180, scale 1:100,000, 3 sheets.

Doelling, H. H., 2002, Geologic map of the Fisher Towers quadrangle, Grand County, Utah: Utah Geological Survey Map 183, scale 1:24,000, 22 sheets.

Doelling, H. H., and T. C. Chidsey, Jr., 2000, Dead Horse Point State Park and vicinity geologic road logs, Grand and San Juan counties, Utah, *in* P. B. Anderson and D. A. Sprinkel, eds., Geologic road, trail, and lake guides to Utah's parks and monuments: Utah Geological Association Publication 29, CD-ROM.

Doelling, H. H., and M. L. Ross, 1998, Geologic map of the Big Bend quadrangle, Grand County, Utah: Utah Geological Survey Map 171, scale 1:24,000, 29 sheets.

Doelling, H. H., M. L. Ross, and W. L. Mulvey, 2002, Geologic map of the Moab quadrangle, Grand County, Utah: Utah Geological Survey Map 181, scale 1:24,000, 34 sheets.

Dubiel, R. F., 1987, Sedimentology of the Upper Triassic Chinle Formation, southeast Utah: Ph.D. thesis, University of Colorado at Boulder, Boulder, Colorado, 132 p.

Dubiel, R. F., J. T. Parrish, J. M. Parrish, and S. C. Good, 1991, The Pangaean megamonsoon— Evidence from the Upper Triassic Chinle Formation, Colorado Plateau: Palaios, v. 6, p. 347–370.

Giles, K. A., and T. F. Lawton, 2002, Halokinetic sequence stratigraphy adjacent to the El Papalote diapir, northeastern Mexico: AAPG Bulletin, v. 86, p. 823–840.

Glennie, K. W., 1987, Desert sedimentary environments, present and past— A summary: Sedimentary Geology, v. 50, p. 135–166.

Goldsmith, P. J., G. Hudson, and P. Van Veen, 2003, Triassic, *in* D. Evans, C. Graham, A. Armour, and P. Bathurst, eds., The millenium atlas: Petroleum geology of the central and northern North Sea: Geological Society (London), p. 105–127.

Gubitosa, R., 1981, Depositional systems of the Moss Back Member, Chinle Formation (Upper Triassic), Canyonlands, Utah: M.S. thesis, Northern Arizona University, Flagstaff, Arizona, 98 p.

Hasiotis, S. T., 2002, Continental trace fossils: SEPM Short Course Notes 51, 132 p.

Hasiotis, S. T., and R. F. Dubiel, 1994, Ichnofossil tiering in Triassic alluvial paleosols: Implications for Pangean continental rocks and paleoclimate, *in* B. Beauchamp, A. F. Embry, and D. Glass, eds., Carboniferous to Jurassic Pangea: Canadian Society of Petroleum Geologists Memoir 17, p. 311–317.

Hasiotis, S. T., and C. E. Mitchell, 1989, Lungfish burrows of the Upper Triassic Chinle and Dolores Formation— Discussion: New evidence suggests origin by a decapod crustacean: Journal of Sedimentary Petrology, v. 59, p. 871–875.

Hasiotis, S. T., C. E. Mitchell, and R. F. Dubiel, 1993, Application of burrow morphologic evaluations: Lungfish or crayfish?: Ichnos, v. 2, p. 315–333.

Hazel, J. E. Jr., 1991, Alluvial architecture of the Upper Triassic Chinle Formation, Cane Creek anticline, Canyonlands, Utah: M.S. thesis, Northern Arizona University, Flagstaff, Arizona, 149 p.

Hazel, J. E. Jr., 1994, Sedimentary response to intrabasinal salt tectonism in the Upper Triassic Chinle Formation, Paradox Basin, Utah: U.S. Geological Survey Bulletin, v. 2000-F, 34 p.

Huntoon, P. W., G. H. Billingsley, Jr., and W. J. Breed, 1982, Geologic map of Canyonlands National Park and vicinity, Utah: Canyonlands Natural History Association, scale 1:62,500, 1 sheet.

Joesling, H. R., J. E. Case, and D. Plouff, 1966, Regional Geophysical investigations of the Moab-Needles area, Utah: U.S. Geological Survey Professional Paper, 516-C, 21 p.

Kelley, V. C., 1958, Tectonics of the region of the Paradox Basin, *in* A. F. Sanborn, ed., Guidebook to the geology of the Paradox Basin: Intermountain Association of Petroleum Geologists, p. 31–38.

Kocurek, G. A., 1996, Desert aeolian systems, *in* H. G. Reading, ed., Sedimentary environments: Processes, facies and stratigraphy, 3d ed.: Oxford, United Kingdom, Blackwell Science, p. 125–153.

Kraus, M. J., 1997, Lower Eocene alluvial paleosols: Pedogenic development, stratigraphic relationships and paleosol-landscape associations: Palaeogeography, Palaeoclimatology, Palaeoecology, v. 129, p. 387–406.

Lawton, T. R., and B. J. Buck, 2006, Implications of diapir-derived detritus and gypsic paleosols in Lower Triassic strata near the Castle Valley salt wall, Paradox Basin, Utah: Geology, v. 34, p. 885–888.

Lucas, S. G., 1993, The Chinle Group: Revised stratigraphy and chronology of Upper Triassic nonmarine strata in the western United States: Museum of Northern Arizona Bulletin, v. 59, p. 27–50.

Lucas, S. G., 1997, Upper Triassic Chinle Group, western United States; a nonmarine standard for Late Triassic time, *in* J. M. Dickens, ed., Late Palaeozoic and early Mesozoic circum-Pacific events and their global correlation: Cambridge, United Kingdom, Cambridge University Press, p. 209–228.

Lucas, S. G., and J. E. Marzolf, 1993, Stratigraphy and sequence stratigraphic interpretation of Upper Triassic strata in Nevada, *in* G. C. Dunn and K. A. McDougall, eds., Mesozoic paleogeography of the western United States— II: Pacific Section SEPM Field Trip Guidebook, v. 71, p. 375–378.

Lucas, S. G., A. B. Heckert, J. W. Estep, and O. J. Anderson, 1997, Stratigraphy, biostratigraphy, and sequence stratigraphy of the Upper Triassic Chinle Group, Four Corners region, *in* O. J. Anderson, B. S. Kues, and S. G. Lucas, eds., Mesozoic geology and paleontology of the Four Corners region: New Mexico Geological Society Guidebook, 48th Field Conference, p. 81–107.

Mack, G. H., and K. A. Rasmussen, 1984, Alluvial-fan sedimentation of the Cutler Formation (Permo-Pennsylvanian), near Gateway, Colorado: Geological Society of America Bulletin, v. 95, p. 109–116.

Martin, C. A. L., and B. R. Turner, 1998, Origins of massive type sandstones in braided river systems: Earth-Science Reviews, v. 44, p. 15–38.

Matthews, W. J., G. J. Hampson, B. D. Trudgill, and J. R. Underhill, 2004, Impact of salt movement on fluvio-lacustrine stratigraphy and facies architecture: Late Triassic Chinle Formation, northern Paradox Basin, SE Utah, U.S.A., *in* P. J. Post, D. L. Olson, K. T. Lyons, S. L. Palmes, P. F. Harrison, and N. C. Rosen, eds., Salt-sediment interactions and hydrocarbon prospectivity: Proceedings of 24th Annual Gulf Coast Section SEPM Foundation Bob F. Perkins Research Conference, p. 931–964.

Miall, A. D., 1978, Lithofacies types and vertical profile models in braided river deposits: A summary, *in* A. D. Miall, ed., Fluvial sedimentology: Canadian Society of Petroleum Geologists Memoir 5, p. 597–604.

Miall, A. D., and M. Arush, 2001, Cryptic sequence boundaries in braided fluvial successions: Sedimentology, v. 48, p. 971–985.

Nuccio, V. F., and S. M. Condon, 1996, Burial and thermal history of the Paradox Basin, Utah and Colorado, and petroleum potential of the middle Pennsylvanian Paradox Formation: U.S. Geological Survey Bulletin, v. 2000-O, 41 p.

Prochnow, S. J., L. C. Nordt, S. C. Atchley, M. R. Hudec, and T. E. Boucher, 2005, Triassic paleosol catenas associated with a salt-withdrawal minibasin in southeastern Utah, U.S.A.: Rocky Mountain Geology, v. 40, p. 25–49.

Prochnow, S. J., L. C. Nordt, S. C. Atchley, and M. R. Hudec, 2006a, Multi-proxy paleosol evidence for Middle and Late Triassic climate trends in eastern Utah: Palaeogeography, Palaeoclimatology, Palaeoecoloy, v. 232, p. 53–72.

Prochnow, S. J., S. C. Atchley, T. E. Boucher, L. C. Nordt, and M. R. Hudec, 2006b, The influence of salt withdrawal subsidence on palaeosol maturity and cyclic fluvial deposition in the Upper Triassic Chinle Formation: Castle Valley, Utah: Sedimentology, v. 53, p. 1319–1345.

Prommel, H. W. C., 1923, Geology and structure of portions of Grand and San Juan counties, Utah: AAPG Bulletin, v. 7, p. 384–399.

Retallack, G. J., 2001, Soils of the past: An introduction to paleopedology, 2d ed.: Oxford, United Kingdom, Blackwell Science, 404 p.

Rowan, M. G., T. F. Lawton, K. A. Giles, and R. A. Ratliff, 2003, Near-salt deformation in La Popa Basin, Mexico, and the northern Gulf of Mexico; a general model for passive diapirism: AAPG Bulletin, v. 87, p. 733–756.

Shelley, D. C., and T. F. Lawton, 2005, Sequence stratigraphy of tidally influenced deposits in a salt-withdrawal minibasin: Upper sandstone member of the Potrerillos Formation (Paleocene), La Popa Basin, Mexico: AAPG Bulletin, v. 89, p. 1157–1179.

Shoemaker, E. M., and W. L. Newman, 1959, Moenkopi Formation (Triassic) in salt anticline region, Colorado and Utah: AAPG Bulletin, v. 43, p. 1835–1851.

Smith, R. I., M. Hodgson, and M. Fulton, 1993, Salt control on Triassic reservoir distribution, UKCS Central North Sea, *in* J. R. Parker, ed., Petroleum geology of northwest Europe: Proceedings of the 4th Conference, Geological Society (London), p. 547–557.

Stevenson, G. M., and D. L. Baars, 1986, The Paradox; a pull-apart basin of Pennsylvanian age, *in* J. A. Peterson, ed., Paleotectonics and sedimentation in the Rocky Mountains region, United States: AAPG Memoir 41, p. 513–539.

Stewart, J. H., 1969, Major Upper Triassic lithogenetic sequences in the Colorado Plateau region: AAPG Bulletin, v. 53, p. 1866–1879.

Stewart, J. H., G. A. Williams, H. F. Albee, and O. B. Raup, 1959, Stratigraphy of Triassic and associated formations in part of the Colorado Plateau region: U.S. Geological Survey Bulletin, v. 1046-Q, p. 487–576.

Stewart, J. H., F. G. Poole, and R. F. Wilson, 1972, Stratigraphy and origin of the Triassic Chinle Formation and related Upper Triassic strata in the Colorado Plateau region: U.S. Geological Survey Professional Paper 690, 336 p.

Stewart, S. A., and J. A. Clark, 1999, Impact of salt on the structure of the central North Sea hydrocarbon fairways, *in* A. J. Fleet and S. A. R. Boldy, eds., Petroleum geology of northwest Europe: Proceedings of the 5th conference, Geological Society (London), p. 179–200.

Talbot, M. R., and P. A. Allen, 1996, Lakes, *in* H. G. Reading, ed., Sedimentary environments: Processes, facies and stratigraphy, 3d ed.: Oxford, United Kingdom, Blackwell Science, p. 83–124.

Taylor, A. M., and R. Goldring, 1993, Description and analysis of bioturbation and ichnofabric: Journal of the Geological Society (London), v. 150, p. 141–148.

Thomas, D. S. G., 1997, Reconstructing ancient arid environments, *in* D. S. G. Thomas, ed., Arid zone geomorphology; process, form and change in drylands, 2d ed.: Chichester, United Kingdom, John Wiley and Sons, p. 577–605.

Trudgill, B. D., N. Banbury, and J. R. Underhill, 2004, Salt evolution as a control on structural and stratigraphic systems: Northern Paradox foreland basin, SE Utah, U.S.A., *in* P. J. Post, D. L. Olson, K. T. Lyons, S. L. Palmes, P. F. Harrison, and N. C. Rosen, eds., Salt-sediment interactions and hydrocarbon prospectivity: Proceedings of 24th Annual Gulf Coast Section SEPM Foundation Bob F. Perkins Research Conference, p. 669–700.

Tyler, N., and F. G. Etheridge, 1993, Depositional setting of the Salt Wash Member of the Morrison Formation, southwest Colorado: Journal of Sedimentary Petrology, v. 53, p. 67–82.

Van Wagoner, J. C., H. W. Posamentier, R. M. Mitchum, P. R. Vail, J. F. Sarg, T. S. Loutit, and J. Hardenbol, 1988, An overview of the fundamentals of sequence stratigraphy and key definitions, *in* C. K. Wilgus, B. S. Hastings, C. G. St. C. Kendall, H. W. Posamentier, C. A. Ross, and J. C. Van Wagoner, eds., Sea-level changes— An integrated approach: SEPM Special Publication 42, p. 39–45.

Vendeville, B. C., and M. P. A. Jackson, 1991, Deposition, extension, and the shape of downbuilding diapirs: AAPG Bulletin, v. 75, p. 687–688.

Volozh, Y., C. J. Talbot, and A. Ismail-Zadeh, 2003, Salt structures and hydrocarbons in the Precaspian Basin: AAPG Bulletin, v. 67, p. 313–334.

White, M. A., and M. I. Jacobson, 1983, Structures associated with the southwest margin of the ancestral Uncompahgre uplift, *in* W. R. Averett, ed., Northern Paradox Basin— Uncompahgre uplift: Grand Junction Geological Society Guidebook, p. 33–39.